

## Overview

# Animal Models for the Study of SARS-CoV-2–induced Respiratory Disease and Pathology

Jacob A Dillard,<sup>1</sup> Sabian A Martinez,<sup>2</sup> Justin J Dearing,<sup>3</sup> Stephanie A Montgomery,<sup>2,4</sup> and Victoria K Baxter<sup>2,4,\*</sup>

Emergence of the betacoronavirus SARS-CoV-2 has resulted in a historic pandemic, with millions of deaths worldwide. An unprecedented effort has been made by the medical, scientific, and public health communities to rapidly develop and implement vaccines and therapeutics to prevent and reduce hospitalizations and deaths. Although SARS-CoV-2 infection can lead to disease in many organ systems, the respiratory system is its main target, with pneumonia and acute respiratory distress syndrome as the hallmark features of severe disease. The large number of patients who have contracted COVID-19 infections since 2019 has permitted a detailed characterization of the clinical and pathologic features of the disease in humans. However, continued progress in the development of effective preventatives and therapies requires a deeper understanding of the pathogenesis of infection. Studies using animal models are necessary to complement *in vitro* findings and human clinical data. Multiple animal species have been evaluated as potential models for studying the respiratory disease caused by SARS-CoV-2 infection. Knowing the similarities and differences between animal and human responses to infection is critical for effective translation of animal data into human medicine. This review provides a detailed summary of the respiratory disease and associated pathology induced by SARS-CoV-2 infection in humans and compares them with the disease that develops in 3 commonly used models: NHP, hamsters, and mice. The effective use of animals to study SARS-CoV-2–induced respiratory disease will enhance our understanding of SARS-CoV-2 pathogenesis, allow the development of novel preventatives and therapeutics, and aid in the preparation for the next emerging virus with pandemic potential.

**Abbreviations:** ACE2, angiotensin-converting enzyme 2; AGM, African green monkey; ALI, acute lung injury; ARDS, acute respiratory distress syndrome; BALF, bronchoalveolar lavage fluid; CARDS, COVID-19-associated acute respiratory distress syndrome; DAD, diffuse alveolar damage; dpi, days postinfection; GGO, ground glass opacities; S, spike glycoprotein

DOI: 10.30802/AALAS-CM-22-000089

## Introduction

As of July 2022, infection with SARS-CoV-2, the betacoronavirus responsible for the COVID-19 pandemic, has caused over 90 million cases and more than 1 million deaths in the United States.<sup>53</sup> Although the virus can affect multiple organ systems, it mainly targets the respiratory system. SARS-CoV-2 infection typically begins in the upper respiratory tract and may progress to pulmonary infection.<sup>52,95</sup> Most COVID-19 infections result in mild to moderate disease.<sup>10,95,160,185</sup> However, in severe cases, pulmonary infection causes interstitial pneumonia, damage and dysfunction of alveolar capillaries, and acute respiratory distress. Pulmonary infection, severe inflammation, and hypoxemia can lead to extrapulmonary disease, including systemic inflammation, coagulopathy, vasculopathy, and multiorgan dysfunction and failure.<sup>10,16,81,95,160,176,183,186</sup>

The primary animal species used to study SARS-CoV-2 infection and disease are NHP, hamsters, and mice.<sup>120</sup> Each species has strengths and weaknesses with regard to capturing important elements of COVID-19 pulmonary disease. Here we detail the current understanding of SARS-CoV-2–induced respiratory disease and pathology in humans and the analogous features seen in each of these 3 species. Knowing which features of human COVID-19 are modeled by these 3 species is critical to designing preclinical experiments that will effectively translate to humans.

## Pathophysiology of SARS-COV-2 Infection in the Human Lung

Viral infection typically begins in the upper respiratory tract. The SARS-CoV-2 spike (S) glycoprotein binds to the receptor for angiotensin-converting enzyme 2 (ACE2) on the surface of respiratory epithelial cells throughout the respiratory tract, including ciliated nasal, oropharyngeal, and tracheal cells; submucosal glands; and bronchial and bronchiolar epithelium.<sup>3,77-79,95,152,198</sup> Host proteases, including the transmembrane protease serine protease 2, process S to promote fusion of the viral and cellular membranes, which in turn allows the SARS-CoV-2 genome to enter the cytosol

Submitted: 28 Jul 2022. Revision requested: 11 Aug 2022. Accepted: 22 Aug 2022.

<sup>1</sup>Department of Microbiology and Immunology, <sup>2</sup>Division of Comparative Medicine, <sup>3</sup>Biological and Biomedical Sciences Program, Office of Graduate Education, and <sup>4</sup>Department of Pathology and Laboratory Medicine, University of North Carolina at Chapel Hill, Chapel Hill, North Carolina

\*Corresponding author: vkbaxter@med.unc.edu

and initiate structural protein translation and viral genome replication. Multiple processes promote the dissemination of infectious viral particles to the lower respiratory tract, where SARS-CoV-2 primarily infects type II alveolar epithelial cells (pneumocytes).<sup>78,79,95,96</sup>

SARS-CoV-2 infection of the lower respiratory tract causes viral interstitial pneumonia that results in widespread acute lung injury (ALI) and pulmonary inflammation that progress to respiratory distress (Figure 1).<sup>10,28,52,61,79,95,160,176</sup> Direct viral and indirect inflammatory damage to both pneumocytes and pulmonary capillary endothelial cells drives disruption of the alveolar–capillary barrier, resulting in increased pulmonary vascular permeability, alveolar edema, and atelectasis. In addition, local inflammation and endothelial injury promote hypercoagulation, which leads to microvascular thrombosis and pulmonary vascular occlusion.<sup>10,28,52,61,79,95,160,176</sup> These pathologic changes lead to reductions in pulmonary compliance and aeration of pulmonary tissue, ventilation–perfusion mismatch, impaired pulmonary gas exchange, and ultimately hypoxemia leading to tissue hypoxia.<sup>10,28,52,61,79,95,160,176</sup> Disruption of the pulmonary alveolar–capillary barrier and microvasculature promotes the reduction of pulmonary gas exchange, which can manifest as acute respiratory distress syndrome (ARDS). A defining feature of ARDS is hypoxemia, which ultimately causes tissue hypoxia, multiorgan dysfunction, and possibly death.<sup>10,52,61,95,128,160,176</sup> Active viral replication is likely to have limited significance during severe disease that occurs later in the infection; severe disease occurs primarily due to systemic hyperinflammation and resulting disease, including coagulopathy and reduced pulmonary function. Local

pulmonary inflammation, vascular injury, and thromboembolic disease may accelerate systemic disease by causing dysregulated feed-forward cascades, including cytokine release syndrome, systemic inflammatory response syndrome ('cytokine storm'), and disseminated intravascular coagulation.<sup>2,95,128,186</sup>

### SARS-CoV-2–induced Disease in Humans

The presentation and clinical course of SARS-CoV-2 infection are extremely variable in human patients. The incubation period typically ranges from 2 to 7 d post infection (dpi).<sup>98</sup> Fever, fatigue, and dry cough are the most common symptoms, whereas dyspnea is the hallmark of moderate and severe disease.<sup>39,81</sup> Other symptoms include sore throat, headache, myalgia, chills, congestion, rhinorrhea, ageusia, anosmia, hemoptysis, nausea, vomiting, and diarrhea.<sup>16,39,73,81,172</sup> Moderate to severe disease that requires hospitalization and ventilatory support generally occurs approximately 1 wk after the onset of symptoms.<sup>16,63</sup> Patients who report dyspnea often exhibit tachypnea.<sup>16,39,73,81</sup>

Although extrapulmonary disease is common in severe COVID-19 infection, the respiratory system is the primary organ system affected by SARS-CoV-2. Most patients experience mild to moderate disease in the upper respiratory tract, but a considerable minority develop severe disease that can include acute respiratory distress, extrapulmonary involvement, and multiorgan failure.<sup>10,95,160,185</sup> Severe COVID-19 infection commonly results in ARDS, which is defined as the acute onset of dyspnea, hypoxemia, and radiologic findings of bilateral

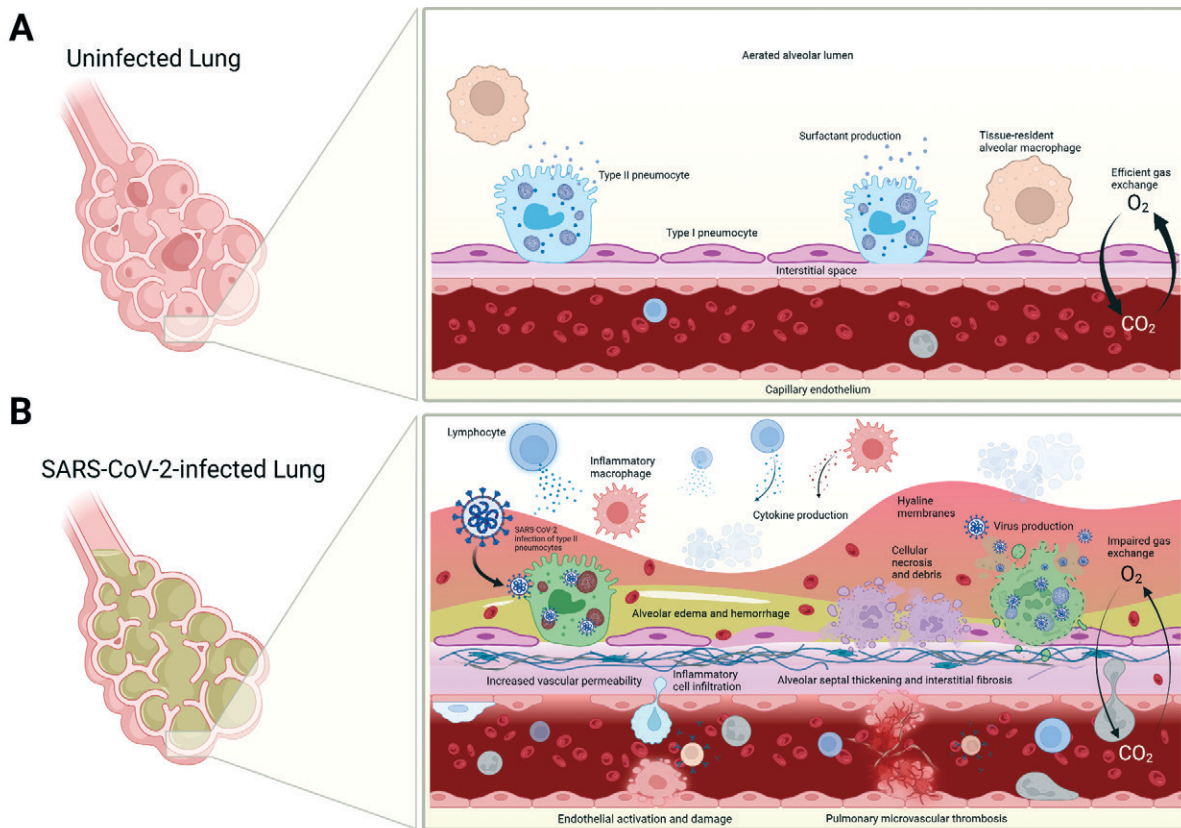


**Figure 1.** Pathophysiology of SARS-CoV-2 infection in the lung. (A) Healthy, uninfected lung with efficient gas exchange between the alveolar lumen and capillary. (B) SARS-CoV-2–infected lung with increased inflammatory infiltrates and cytokine production, alveolar edema and hemorrhage, cellular necrosis and luminal debris, hyaline membrane formation, endothelial activation and damage leading to increased vascular permeability, and microvascular thromboses—all of which contribute to impaired gas exchange.

infiltrates that occur within 1 wk of an identified insult (for example, infection or trauma) and that cannot be explained by cardiac complications or fluid overload.<sup>6,10</sup> Hypoxemia, characterized as a blood oxygen saturation of 93% or less, is a defining feature of severe COVID-19 infection<sup>16,183</sup> and may present in the absence of dyspnea (a condition often referred to as ‘happy hypoxia’).<sup>38,187,200</sup> Hypercapnia is reported also.<sup>160</sup> The most common cause of death is hypoxic multiorgan failure secondary to ARDS and respiratory failure.<sup>16,81</sup> Risk factors for severe disease include advanced age, male sex, smoking, and several comorbidities, including hypertension, diabetes mellitus, coronary artery disease, and chronic pulmonary disease.<sup>16,54,63,81,137,183</sup>

Compared with ARDS precipitated by other causes, COVID-19–associated ARDS (CARDS) commonly involves vascular endothelial injury, coagulopathy, and consequent dysfunctional pulmonary perfusion.<sup>2,64,75,125</sup> Furthermore, a subset of patients exhibits the atypical ARDS phenotype of severe hypoxemia without reduced pulmonary compliance.<sup>64</sup> Although some consider CARDS to be a distinct disease,<sup>10,64</sup> the current expert consensus is that it is broadly similar to and overlaps with the pathophysiology of general ARDS and is therefore a subtype of ARDS. The atypical CARDS phenotype seen in some patients may be a transitional pathophysiologic state that occurs before progression to classic ARDS.<sup>74,124,130,160</sup>

Similar to classic ARDS, severe COVID-19 infection and CARDS commonly present with pulmonary function abnormalities that include low compliance, increased lung weight, a low ventilation–perfusion ratio, reduced lung gas volume, and high recruitability (of unaerated pulmonary tissue).<sup>10,59,70,93,130,160,200</sup> Consistent with frequent reports of COVID-19–associated pulmonary fibrosis, one study reported reduced inspiratory vital capacity, indicating restriction, in patients with CARDS.<sup>12,17,25,60,102,134,149,174</sup> Dysregulation of normal pulmonary perfusion (for example, via loss of adaptive hypoxic vasoconstriction), can result in maladaptive/pathologic perfusion of unaerated tissue,<sup>8,9,64,74</sup> and mild pulmonary hypertension is reported often.<sup>31,57,129,160</sup> Severe COVID-19 infections are associated with long-term impairment of pulmonary function, as indicated by reduced diffusion capacity; a meta-analysis of pulmonary function in recovering COVID-19 patients found reduced carbon monoxide diffusion capacity ( $DL_{CO}$ ).<sup>164</sup>

Several studies have demonstrated the utility of radiologic imaging in both prognosis and investigation of the pathophysiology of severe COVID-19 infection. Despite occasional negative radiologic imaging findings in patients with moderate to severe disease,<sup>80</sup> patients usually present with imaging findings indicative of interstitial pneumonia and vascular abnormalities. Chest X-rays and computed tomography (CT) often reveal diffuse, bilateral ground-glass opacities (GGO), predominantly in peripheral, basilar, and posterior lung regions; these progress to consolidations over the course of the disease.<sup>15,39,73,81,172,180</sup> CT further demonstrates GGO, air bronchograms, ‘crazy paving’ patterns, interlobular and interstitial thickening, frequent pulmonary embolism, vascular abnormalities that include congestion and filling defects, and occasional pleural effusions.<sup>8,9,11,15,29,147,153</sup> Pulmonary scintigraphy of the conducting airways shows intense tracer uptake, indicating tracheobronchitis.<sup>169</sup> Dual-energy CT and CT angiography show correlations between GGO, pulmonary perfusion defects, and abnormal coagulation parameters, such as D-dimer levels, indicating severe disease.<sup>70,97,145</sup> Dual-energy CT has revealed high perfusion of areas of GGO and consolidation, suggesting loss of physiologic hypoxic vasoconstriction.<sup>97,132,160</sup> Using paired analysis of

matched postmortem pulmonary samples, one group correlated CT imaging findings with histopathologic patterns of diffuse alveolar damage (DAD); GGO were associated with exudative DAD, crazy paving patterns with proliferative (or organizing) DAD, and consolidation with fibrosis.<sup>12</sup>

CBC analysis in COVID-19 patients often reveals neutrophilia, including increased numbers of immature neutrophils, and lymphopenia.<sup>39,73,81,172</sup> Other abnormal peripheral blood immune cell parameters include a relative increase in T cells, monocytes, NK cells, and neutrophils exhibiting upregulated activation states.<sup>111,141,177,184</sup> COVID-19 infection is associated with numerous blood indicators of inflammation, including elevated C-reactive protein, erythrocyte sedimentation rate, ferritin, procalcitonin, bradykinin, and IL1, IL6, IL8, and  $TNF\alpha$ .<sup>39,107,167,183</sup> Coagulation abnormalities and vascular endothelial cell dysfunction are common also.<sup>2,39,70,73,101,142,161,170,201</sup>

Bronchoalveolar lavage fluid (BALF) commonly contains viral RNA<sup>14,66</sup> and elevated cellularity, including monocytosis and lymphocytosis (mostly  $CD4^+$  and  $CD8^+$  T cells but also plasmacytes).<sup>14,65,66,69,171</sup> Some groups have reported low T-cell counts associated with severe disease.<sup>45,103</sup> Monocyte-derived inflammatory macrophages drive BALF monocytosis, and tissue-resident alveolar macrophage numbers are reduced markedly.<sup>41,103,173</sup> Evidence of SARS-CoV-2 infection of and replication within monocyte-derived inflammatory macrophages and blood monocytes has been reported.<sup>69,87</sup> However, one group reported that infected blood monocytes and macrophages abort infection and do not produce infectious virions.<sup>87</sup> Infiltrating lymphocytic and monocytic cells show highly activated phenotypes.<sup>14,65,66,69,194</sup> Although not as common as in other types of ARDS, a subset of patients exhibits elevated neutrophil levels in BALF; this finding may depend on the timing of specimen collection relative to symptom onset or initiation of ventilatory support.<sup>14,69,170,199</sup> Single-cell transcriptomic analysis of BALF cell populations reveals upregulation of proinflammatory cytokine and chemokine genes, including *Ccl2*, *Ccl7*, *Ccl8*, *Ccl13*, *Cxcl10*, *Il1b*, *Il8*, and *Tnfr*,<sup>41,45,69,194</sup> IFN-stimulated genes, and complement activation.<sup>45,69,194,199</sup> However, IL6 levels are occasionally relatively low.<sup>69,170</sup> Low BALF: blood ratios of several proinflammatory cytokines, including IL6, may reflect the decompartmentalization or systemic release of pulmonary cytokines.<sup>170</sup> Pleural effusion may occur during severe disease, with lymphocytosis, histiocytosis, hemophagocytosis, and occasional atypical mesothelial cells.<sup>29,30</sup> Elevated levels of vasoactive eicosanoids and vascular endothelial growth factor may also be present, indicating endothelial injury.<sup>170</sup> Cellular analysis of nasopharyngeal and pharyngeal specimens from patients with severe disease showed the infiltration of neutrophils and monocyte-derived inflammatory macrophages and upregulation of proinflammatory cytokines.<sup>41</sup>

## SARS-CoV-2–induced Lung Pathology in Humans

Postmortem respiratory histopathology from COVID-19 patients is heavily biased toward later and more severe disease, and as such, several important caveats should be understood. Potential confounding factors include comorbidities, superinfection, iatrogenic insults like mechanical ventilation, and postmortem autolytic changes.<sup>21,118</sup> Furthermore, most autopsy studies are performed at single institutions and do not compare findings with controls or reference specimens (for example, specimens obtained from healthy tissue or other pulmonary



disease, including other types of viral interstitial pneumonia).<sup>86</sup> Most COVID-19 postmortem respiratory specimens show histopathologic changes similar to ARDS caused by other insults, and therefore are not pathognomonic.<sup>91</sup> Finally, a major characteristic of COVID-19 respiratory pathology is spatial and temporal heterogeneity, which complicates the ability to provide universal characterization.<sup>20,25,28,29,49,116,118</sup>

Gross examination of COVID-19 postmortem respiratory tissue demonstrates increased lung weight, foci of infarction and hemorrhage, extensive congestion and edema,<sup>15,25,60,99</sup> pulmonary arterial thrombosis, and pulmonary embolism and infarction.<sup>20,25,75,99</sup> Occasionally pleural effusion is reported also.<sup>29,99</sup> SARS-CoV-2 RNA and protein are detected in epithelia throughout the majority of the respiratory tract, including epithelia of the conducting airways and both type I and II pneumocytes, as well as within pulmonary endothelial cells, alveolar macrophages, and hyaline membranes.<sup>22,109,123,146,188,192</sup> Postmortem histopathology of the conducting airways demonstrates upper respiratory tract inflammation, including pharyngeal, tracheal, bronchial, and bronchiolar lymphocytic and neutrophilic infiltration and edema.<sup>13,15,20,25,60,115,119,150,169</sup>

The central histopathologic feature in the lungs of COVID-19 patients is DAD. Exudative DAD is present for about 7 to 14 d after symptom onset and includes hyaline membranes, epithelial damage and necrosis, pneumocyte necrosis and desquamation, alveolar edema, and alveolar septal thickening.<sup>2,20,25,29,34,109,126,186,192</sup> Postmortem analysis also reveals signs of proliferative (or organizing) DAD, including hyperplasia of type II pneumocytes and myofibroblasts, atypical pneumocytes, alveolar fibrin deposition, and extracellular matrix deposition.<sup>20,25,29,34</sup> One group reported an elevated number of type II pneumocytes with a dysfunctional transitional phenotype, referred to variously in the literature as preAT1 transitional cells, damage-associated transient progenitors, and alveolar differentiation intermediates.<sup>113</sup> Viral cytopathic effects, including multinucleated cells and viral inclusion bodies, are reported occasionally.<sup>60,133,163,192</sup>

Vasculopathy and thromboembolic pathology are more frequent in CARDS compared with other causes of ARDS, including influenza.<sup>2,75,125</sup> Pulmonary vascular pathology and coagulopathy are indicated by endothelial damage and necrosis, vasculitis including capillaritis, capillary microthrombosis, alveolar fibrin deposition, alveolar hemorrhage, vascular congestion, arterial and venous thromboembolism, and angiogenesis.<sup>2,20,25,99,115,168,175,186</sup> Some studies report acute fibrinous organizing pneumonia, in which extensive alveolar fibrin deposition is a hallmark histopathologic description.<sup>91,116</sup>

Light microscopy demonstrates lymphocytic perivascular infiltrates and a mononuclear, primarily lymphocytic, interstitial infiltrate.<sup>2,15,25,34,60,115,163</sup> Immunohistochemistry staining indicated that the infiltrating lymphocytes were primarily CD4<sup>+</sup> and CD8<sup>+</sup> T cells,<sup>60</sup> whereas single-cell transcriptomic analysis found no evidence of an increase in T cells in pulmonary tissue, suggesting the lymphocytes detected by histopathology may mostly be NK cells.<sup>47,95</sup> Some groups have reported that macrophages predominate in the alveolar space.<sup>34,134</sup> One group found evidence of increased dendritic cells and macrophages by transcriptomic analysis of postmortem pulmonary tissue, whereas another group using the same method reported a high frequency of aberrantly activated monocyte-derived inflammatory and tissue-resident alveolar macrophages.<sup>47,113</sup>

Although not reported as commonly in CARDS as in general ARDS, a predominantly neutrophilic infiltrate, leading to neutrophilic capillaritis and present within alveoli and

tracheal mucosal interstitium, is detected occasionally. This infiltrate is sometimes interpreted as resulting from superinfection.<sup>13,20-22,34,115,163</sup> Neutrophils in microthrombi and neutrophil extracellular traps also appear to be involved in vascular and thromboembolic pathology.<sup>117,125,126,135</sup> Some reports indicate occasional histopathologic signs of both bacterial and fungal infection.<sup>20,56,71,82,115,175</sup> Other signs of inflammation include multinucleated interstitial cells<sup>25,29</sup> and elevated proinflammatory cytokine production (for example, IL1, IL6, TNF $\alpha$ , and CXCL10).<sup>105</sup>

Pulmonary specimens obtained during late-stage or postacute disease show fibrotic changes and tissue remodeling, including continued interstitial extracellular matrix deposition, fibroblast and myofibroblast hyperplasia, and intraalveolar fibrous material.<sup>12,17,25,60,102,149</sup> CARDS patients also show evidence of fibroproliferative disease, including extensive histopathologic indications of tissue remodeling, a profibrotic gene expression and proteomic profile in monocyte-derived macrophages, and signs of restrictive pulmonary mechanics.<sup>174</sup> In addition, COVID-19-associated fibrotic changes can occur simultaneously in acute and subacute disease.<sup>134</sup>

Pathologic analysis of pulmonary specimens has contributed enormously to our understanding of the pathophysiology of COVID-19. However, relatively few premortem lung biopsies have been taken from patients due to safety risks, including the frequently critical condition of patients and risk of infectious exposure.<sup>29,62</sup> Histopathology of transtracheal and transbronchial biopsies indicate interstitial pneumonia with lymphocytic and monocytic infiltrates, exudative and proliferative (or organizing) DAD, and endothelialitis.<sup>89,133,162,195</sup> Biopsy specimens obtained earlier in infection show less vasculopathy.<sup>133,160,163</sup> Evaluation of transudative pleural effusion fluid has revealed lymphocytosis, histiocytosis, hemophagocytosis, and occasional atypical mesothelial cells; viral cytopathic effects have not been observed, and SARS-CoV-2 RNA has been undetectable.<sup>30</sup> Compared with postmortem biopsies, which are systematically biased toward late stage and critical disease, *in vivo* respiratory tract biopsies from patients with severe disease will be crucial to advancing knowledge of pathologic characteristics of SARS-CoV-2 infection in humans.

## NHP as Models of SARS-CoV-2-induced Respiratory Disease and Lung Pathology

Several NHP species have been used to study COVID-19, the most common of which are rhesus macaques (*Macaca mulatta*), cynomolgus macaques (*Macaca fascicularis*), and African green monkeys (AGM, *Chlorocebus aethiops*); we will also discuss hamadryas baboons (*Papio hamadryas*) and common marmosets (*Callithrix jacchus*). NHP exhibit a high degree of genetic, anatomic, physiologic, and immunologic similarity to humans and closely reflect the human cellular expression profile and amino-acid sequence of ACE2.<sup>5,43,165,179</sup> However, NHP models have several limitations, including high costs and labor, low supply of animals relative to demand, and ethical issues. Furthermore, NHP experiments involve low sample sizes and often lack standardization of experimental design and reporting.<sup>37,43,158,165,179</sup> Nonetheless, these animals are indispensable for understanding SARS-CoV-2 pathogenesis and for the development and assessment of prophylactic and therapeutic measures against COVID-19.

Like humans, NHPs usually develop asymptomatic infections and mild to moderate clinical disease with high interindividual variability.<sup>18,36,37,44,46,58,76,121,138,144,151,155,165,182</sup>

With the exception of 4 aged AGM used in 2 studies,<sup>19,58</sup> NHP do not develop severe clinical disease or acute respiratory distress syndrome.<sup>36,48,106,121,138,182,190</sup> Several reports indicate that more severe pulmonary disease, higher viral burden, and prolonged virus shedding occur in aged NHP.<sup>19,138,155,166,190</sup> Currently, the incidence of severe disease is not different in male and female NHP.

A meta-analysis of studies using rhesus macaques, cynomolgus macaques, and AGM revealed similar disease parameters, including early blood leukocytosis and prolonged interstitial pneumonia, in all 3 species. However, the clinical presentation in these 3 species was significantly different from that in humans, with rhesus macaques providing a potentially superior model.<sup>179</sup> Compared with cynomolgus macaques and common marmosets, rhesus macaques provided a superior model of mild to moderate COVID-19.<sup>106</sup> However, despite similar viral lung titers, AGM and baboons showed more indications of severe disease than did age-matched rhesus macaques.<sup>19,155,182</sup> Common marmosets appear to be relatively resistant to both SARS-CoV-2 infection and clinical disease.<sup>106,155</sup>

NHP show viral shedding is detected throughout the respiratory tract, including nasal, oropharyngeal, tracheal, bronchial, and pulmonary tissue.<sup>18,19,36,44,46,48,68,76,85,106,121,138,144,151,155,166,182,190,196</sup> Viral replication in the upper respiratory tract peaks at 1 to 3 dpi, whereas in the lower respiratory tract, viral levels peak later and commonly persist through 14 to 18 dpi.<sup>19,106,138,151,155,156,182,190,196</sup> In addition, the time course of clinical disease is similar in humans and NHP, persisting for approximately 8 to 16 d in rhesus macaques.<sup>121,151</sup> Common clinical signs in most NHP species include fever,<sup>18,44,46,58,76,84,85,92,106,121,138,151,155,156,166,182,196</sup> reduced appetite,<sup>19,36,44,48,58,84,121,138,151,157,182,196</sup> mild weight loss,<sup>48,84,106,121,151,155,156,166,190</sup> and lethargy.<sup>92,190,196</sup> Clinical presentation can also include dehydration,<sup>58,121,138,151</sup> hunched posture,<sup>48,121,157</sup> piloerection,<sup>121</sup> pallor,<sup>121,138,151</sup> ocular erythema,<sup>85</sup> and rhinorrhea.<sup>138,182</sup> Important indications of respiratory disease include occasional apparent dyspnea (evident by abdominal effort and nasal flaring),<sup>19,85</sup> and increased respiratory sounds by auscultation.<sup>85</sup> In contrast to humans, coughing occurs only occasionally in NHP<sup>58,85,121,196</sup> but tachypnea is common,<sup>19,48,58,85,121,157</sup> and irregular respiratory rate has been reported in some rhesus macaque studies.<sup>121,138,151</sup> Tachycardia has been reported in rhesus macaques, cynomolgus macaques, and AGM.<sup>85</sup> Finally, hypothermia, which has been reported in several NHP studies, sometimes correlates with severe disease.<sup>19,58,76</sup>

Overt respiratory distress and reduced pulmonary function are rarely reported in NHP. For example, a 2020 systematic review did not find acute hypoxemic respiratory failure, extrapulmonary dysfunction, or lethal disease in any NHP.<sup>55</sup> Despite frequent relatively severe pulmonary pathology and radiologic findings (discussed later), NHP more commonly show mild to moderate clinical disease and therefore are not ideal models for CARDS. Despite these limitations, several publications indicate the potential for NHP to model severe disease with hypoxemic respiratory distress.<sup>19,48,58,76,85,121,138,151,157</sup> In particular, severe disease with respiratory distress that required euthanasia was described in aged AGM.<sup>19,58</sup> Furthermore, dyspnea and tachypnea or irregular respiration was seen in rhesus macaques, cynomolgus macaques, and AGM.<sup>19,48,58,85,121,138,151,157</sup> Another study detected a transient reduction in pulmonary tidal volume in AGM.<sup>76</sup> Finally, pulse oximetry has occasionally detected hypoxemia, including severe hypoxemia that corresponds to lethal disease, in aged NHP.<sup>19,58,85</sup>

Similar to those in humans, thoracic radiologic findings in most NHP commonly indicate interstitial pneumonia. Chest X-rays and CT reveal bilateral diffuse pulmonary infiltrates including GGO and consolidation,<sup>18,19,48,58,76,84,85,106,121,151,156,158,165,166,182,190</sup> predominantly in peripheral and caudal pulmonary regions.<sup>84,121,144</sup> Vascular abnormalities and crazy paving patterns are often detected by CT.<sup>23,76,85,108,144,155,190</sup> Chest radiography revealed diffuse alveolar patterns in 2 studies that found severe disease in aged AGM.<sup>19,58</sup> Consistent with a lack of other clinical indications, common marmosets did not demonstrate pulmonary radiologic signs, which were more severe in rhesus macaques than in cynomolgus macaques.<sup>106</sup> Residual pulmonary lesions were present until as late as 38 dpi, after the resolution of acute disease.<sup>23</sup> An extensive review of the various imaging modalities used for SARS-CoV-2 models in NHP found that mild to moderate lung disease is detected consistently in most infected NHP species but that severe radiologic abnormalities are uncommon.<sup>158</sup> Compared with chest X-rays, CT is considered to be a more sensitive method for detecting radiologic abnormalities in NHP,<sup>158,165</sup> and radiography correlates well with gross pathologic and histopathologic findings.<sup>158</sup>

Blood analysis confirms inflammatory cellular responses in most NHP species. Monocytosis, neutrophilia, and lymphopenia are the most common findings,<sup>36,44,76,84,85,92,106,121,182,190</sup> with some reports of lymphocytosis, neutropenia, leukopenia, and reduced NK cells.<sup>36,58,94,106,121,151,166,196</sup> The results of CBC analyses appear to depend strongly on the timing of blood collection<sup>44,76,106,121,196</sup> and possibly on the inoculation dose.<sup>36</sup> In particular, one study found that early lymphocytosis and later lymphopenia were likely the result of proliferation and subsequent pulmonary recruitment.<sup>5</sup> Thrombocytopenia and other indications of systemic coagulopathy (including elevated fibrinogen levels, prolonged activated partial thromboplastin time, and up-regulated thrombotic pathways) have been reported by several groups.<sup>4,44,76,85,155,166,182</sup> Rare findings potentially resulting from respiratory dysfunction include hypercapnia and acidosis.<sup>155,156</sup> Finally, several NHP studies have detected regenerative anemia, which is not reported to occur in humans.<sup>85,121,155,182</sup>

NHP also exhibit numerous signs of systemic inflammation and both vascular and respiratory disease. Elevated markers of systemic inflammation include many inflammatory cytokines, chemokines, and acute phase proteins, frequently IL1a, IL1b, IL10, IFN $\alpha$ , IFN $\beta$ , IFN $\gamma$ , IL1RA, TNF $\alpha$ , IP10, MIP1b, MCP1, and C-reactive protein.<sup>4,18,19,36,58,68,76,84,106,108,121,155,156,166,182,196</sup> Levels of IL2, IL4, IL5, IL13, IL15, and CCL11 are also often above baseline.<sup>19,68,76,84,106,155,166,182,196</sup> Consistent with human disease, multiple reports demonstrate the importance of the timing and balance of cytokine production in determining the severity and progression of disease in NHP.<sup>19,58,156</sup>

BALF examination in NHP reveals elevated proinflammatory cytokines, chemokines, and IFN-stimulated genes. IL6 and IL8 are the most commonly reported elevated proinflammatory cytokines, but other elevated factors include IL1b, IL10, IFN $\alpha$ , IFN $\gamma$ , IL1RA, TNF $\alpha$ , IP10, MIP1b, MCP1, and perforin.<sup>4,155,182,196</sup> Monocytosis was reported in 2 studies,<sup>58,182</sup> one of which also reported neutrophilic infiltrates.<sup>58</sup> Transcriptomic analysis of bronchoalveolar lavage cells revealed more severe inflammation in baboons compared to rhesus macaques, and in older baboons compared to younger baboons.<sup>155</sup> In rhesus macaques, younger individuals showed increased type I IFN signaling compared to older individuals.<sup>139</sup> The same method also revealed a correlation between severe disease and inflammatory infiltration, and milder disease was associated with both IL10:IL6 and kynurenine:tryptophan ratios.<sup>58</sup> Single-cell transcriptomics

showed active viral replication in pneumocytes,<sup>157</sup> and transcriptomic analysis of both blood and bronchoalveolar lavage cells indicated upregulation of pathways associated with complement and platelet activation, thrombosis, vascular injury and repair, and neutrophil degranulation.<sup>4,139</sup>

Pathologic examination of the lungs of SARS-CoV-2-infected NHP tends to show mild to moderate pathology overall. Gross examination of infected NHP pulmonary tissue largely corroborates findings in humans, with multifocal to diffuse signs of inflammation, tissue damage, consolidation, hyperemia, and hemorrhage in most NHP species.<sup>19,36,44,84,85,106,121,138,144,156,157,182,196</sup> Focally diffuse hemorrhage was the most common finding on macroscopic examination in one review.<sup>165</sup> One study reported pulmonary edema, detected as increased lung weight relative to body weight in rhesus macaques.<sup>121</sup> Some studies also described hilar or mediastinal lymphadenopathy<sup>18,106,157,165</sup> and occasional pleural adhesions.<sup>18,85,121,196</sup>

Inflammation and tissue damage in the upper respiratory tract and conducting airways are common features in NHP. Rhinitis, tracheitis, bronchitis, and bronchiolitis involve both mononuclear cells and granulocytes. Mucosal epithelial damage and necrosis can coincide with inflammation.<sup>18,36,42,44,121,138,155,156,182</sup> As in humans, NHP show rare multinucleated cells throughout the respiratory tract.<sup>18,19,36,42,58,85,138,155</sup> One study reported upper respiratory tract squamous metaplasia and bronchiolar lymphoid hyperplasia in rhesus macaques.<sup>121</sup> The same group used electron microscopy to observe edematous but intact alveolar epithelial basement membranes in the context of interstitial and alveolar inflammation.<sup>121</sup> Finally, as in humans, rhesus macaques, cynomolgus macaques, and AGM show SARS-CoV-2 antigen extensively throughout the respiratory tract, including in type I and II pneumocytes, upper respiratory tract and conducting airway epithelial cells,<sup>18,36,48,106,121,138,182,190</sup> and alveolar macrophages.<sup>18,121,182,190</sup> One study reported viral antigen detection in pulmonary endothelial cells of AGM.<sup>104</sup>

Although NHP primarily develop only mild clinical signs, they often have moderate to severe pulmonary histopathology. Compared with those of New World NHP species, including common marmosets and squirrel monkeys, Old World Species (rhesus macaques, cynomolgus macaques, AGM, and baboons) typically show more severe histopathologic abnormalities.<sup>42,155</sup> Pulmonary inflammation was more severe in baboons than rhesus macaques, but common marmosets had no major pathologic findings.<sup>155</sup>

The most common histopathologic finding in NHP is multifocal and diffuse interstitial pneumonia of variable severity.<sup>18,19,36,42,44,48,85,92,94,106,121,138,144,151,155,156,182,190,196</sup> Bronchial and bronchiolar involvement is observed occasionally.<sup>58,121,138,144,151,182</sup> Severe DAD with extensive hyaline membrane formation is less common in NHP than in human autopsy reports. However, NHP frequently exhibit less severe alveolar epithelial and interstitial pathology (for example, cellular necrosis and debris, alveolar septal thickening, alveolar edema, alveolar fibrin deposition, and alveolar hemorrhage).<sup>18,19,36,42,48,58,85,106,121,138,151,155,182,190,196</sup> Type II pneumocyte hyperplasia is often reported in NHP.<sup>18,58,85,121,138,182</sup> In addition, NHP appear to model several elements of vasculopathy that are associated with COVID-19, including endothelialitis and vasculitis, pulmonary microthrombi, alveolar hemorrhage, and both intimal smooth muscle and endothelial cellular proliferation.<sup>4,58,84,92,106,151,155,182</sup> However despite common signs of vascular disease, obvious coagulopathy is observed only occasionally.<sup>76,85,155,165,166,182</sup>

The inflammatory infiltrate profile in NHP lungs is similar to that seen in human autopsies. Mononuclear cells consisting of monocytes and T cells predominate in the interstitium and perivascular regions.<sup>18,19,36,44,85,106,121,138,144,151,156,196</sup> Further reflecting the composition of the inflammatory infiltrate in humans, pulmonary neutrophils are present but less frequent in NHP,<sup>19,44,121,138,156</sup> and eosinophils are rarely seen.<sup>44,121,155</sup> Macrophages, including infiltrating monocyte-derived inflammatory macrophages, are common in alveolar lumens.<sup>19,48,121,138,155</sup> One study reported increased elevated peripheral blood neutrophils at 1 dpi and persistent (2 weeks post-infection) elevation of CD8<sup>+</sup> T cells in the lungs of aged rhesus macaques, and another found a correlation between pulmonary CD4<sup>+</sup> T cells and lymphopenia.<sup>156,196</sup> Common marmosets showed only mild pneumonitis as compared with other NHP species.<sup>106,155</sup> Although most NHP necropsies are performed during the acute or subacute disease period, residual pulmonary inflammatory infiltrates have been detected in AGM as long as 5 wk after infection.<sup>76</sup> Fibroproliferative pathology, including alveolar septal thickening and elevated pulmonary collagen deposition, is often noted during early convalescence,<sup>4,18,44,85,121,138,155,156</sup> with fibrosis and type II pneumocyte hyperplasia more frequent in cynomolgus macaques and AGM than in rhesus macaques.<sup>85</sup>

## Hamsters as Models of SARS-CoV-2-induced Respiratory Disease and Lung Pathology

Although NHP exhibit many features of human SARS-CoV-2-induced disease, in-depth pathogenesis studies frequently require a smaller, more cost-effective model. Syrian golden hamsters (*Mesocricetus auratus*) have proven to be a suitable model for studying COVID-19. The natural susceptibility of hamsters is due to the high similarity of their ACE2 amino acid sequence at the receptor binding domain of the SARS-CoV-2 S glycoprotein to that of humans. This feature allows evaluation of human clinical isolates without the need to alter either the virus or recipient animal, and the resulting disease includes many of the characteristics of COVID-19 patients.<sup>35</sup> In addition, hamsters are readily available, relatively inexpensive to house, and generally easy to manage and handle. The sparse availability of hamster-specific laboratory reagents is a key limitation of this model. Furthermore, unlike humans and many other animals, hamsters do not have easily accessible large veins for serial blood sampling, thus limiting evaluation of hematologic, clinical chemistry, and coagulation parameters. Similarly, BALF evaluation of challenged, untreated hamsters is rarely reported, indicating an additional limitation of this species.

The course of infection and rapid viral clearance in hamster models of SARS-CoV-2 infection closely mirror those of humans. Viral antigen and RNA are detected in bronchiolar epithelial cells, type I and II pneumocytes,<sup>40,127,140</sup> and olfactory sensory neurons, basal cells, and sustentacular cells of the olfactory epithelium in the nasal turbinates.<sup>193</sup> Throughout infection in hamsters, viral RNA load and infectious viral titers follow similar timelines in both the lungs and nasal turbinates. Both viral RNA and infectious viral titers peak at 2 dpi, and infectious virus is often below the limit of detection by 7 to 10 dpi.<sup>35,40,50,83,127,140,154,191,193</sup> Viral RNA is typically detectable through 14 dpi or later.<sup>50,127</sup> In addition, young hamsters clear infectious virus and viral RNA faster than aged hamsters.<sup>127</sup> Finally, the long-lasting infection and reduced viral clearance of immunocompromised or immunosuppressed COVID-19 patients can be modeled in immunosuppressed hamsters.<sup>27</sup>



Compared with humans, hamsters display fewer signs of clinical disease and have little to no incubation period after inoculation. The hallmark clinical sign is progressive body weight loss starting at 1 to 2 dpi and typically peaking around 6 to 7 dpi;<sup>35,40,50,83,127,140,191</sup> hamsters are generally fully recovered by 2 to 3 wk after infection.<sup>35,50,83,127,140</sup> Other commonly reported clinical signs include lethargy, weakness, ruffled fur coat or piloerection, hunched posture, and respiratory distress in the form of rapid or labored respiration starting at approximately 2 to 3 dpi.<sup>35,40,140,191</sup> Unlike humans, hamsters do not develop fever or significant changes in body temperature throughout the course of infection.<sup>127,140</sup> In addition, no mortality is reported, except for the rare scenario of an animal reaching humane endpoint criteria due to excessive body weight loss.<sup>83</sup> Inoculation dose plays a large role in disease severity in hamsters. Lower inoculation doses of  $10^3$  pfu often result in fewer clinical symptoms and slower pathology onset but still yield similar viral replication kinetics and pathology by 6 to 7 dpi.<sup>83,140,191</sup> Like humans, hamsters have greater risk of severe disease with advanced age and male sex. Multiple research groups have reported that male hamsters are more susceptible than females to developing clinical disease; males show more severe disease signs, including greater weight loss and longer time to recovery<sup>50,143,191</sup> and show more severe pulmonary damage.<sup>50,143,191</sup> In addition, aged hamsters show worse disease outcomes than do young animals, including greater and more consistent weight loss and more widespread and pronounced pathologic findings.<sup>83,127</sup> However, in one study, neither sex nor age influenced clinical signs, body weight loss, or pathologic findings.<sup>140</sup>

Due to their small size, conventional chest X-rays are not commonly performed in hamsters, but CT and positron emission tomography (PET) are viewed as comparable imaging techniques.<sup>24,50,83,143</sup> Similar to COVID-19 patients, infected hamsters demonstrate bilateral GGO and lung consolidation indicative of interstitial pneumonia.<sup>26</sup> In particular, abnormal  $\mu$ CT findings were found in infected hamsters until 20 dpi; these included transient pneumomediastinum in all animals on study.<sup>83</sup> In addition, PET scans of SARS-CoV-2–infected hamsters that were surgically implanted with central venous catheters showed heavy dye accumulation in pulmonary lesions at 24 h after intravenous injection of  $^{124}\text{I}$ -iodo-DPA-713.<sup>143</sup> These imaging techniques allow disease progression to be monitored in a noninvasive manner.

Hamsters can exhibit a ‘cytokine storm’ after infection with SARS-CoV-2. Proinflammatory cytokines and IFN, including IFN $\gamma$ , IL6, IL10, TNF $\alpha$ , and IFN $\alpha$ , are potentially induced starting at 2 dpi, peak at 4 dpi, and return to baseline by 7 dpi.<sup>35,50,154</sup> In addition, at 7 dpi, TGF $\beta$  levels increase, suggesting resolution of the acute inflammatory response.<sup>35</sup> This cytokine storm is thought to help control infection and reduce viral load but also likely promotes the development of more severe pulmonary pathology.<sup>24</sup> In the nasal turbinates, cytokine expression follows a similar timeline, with abundant expression of proinflammatory cytokines and chemokines that include IL1 $\beta$ , IL6, TNF $\alpha$ , CCL3, CCL5, and CXCL10.<sup>193</sup> In contrast to pulmonary tissue, IFN $\alpha$  and IFN $\gamma$  levels are not significantly elevated in nasal turbinates.<sup>193</sup>

Infected hamsters exhibit gross pulmonary consolidation, with approximately 50% to 60% of the lungs affected by 7 dpi.<sup>35,40</sup> Macroscopic pulmonary findings commonly include large patches of focal inflammation, pulmonary edema, intense red and brown lung discoloration, increased lung weight and lung-to-body weight ratios, and interstitial pneu-

monia.<sup>35,40,143,154,191</sup> These features closely mirror many of the hallmark gross findings present in COVID-19 patients.

Comparable to COVID-19 in humans, DAD is the main histopathologic feature of SARS-CoV-2 infection in hamsters. Evidence of DAD can be seen as early as 2 dpi, with peak damage at 5 to 6 dpi, and evidence of resolution by 10 to 14 dpi. Elements of DAD seen in hamsters are very similar to those of humans, including alveolar epithelial damage and necrosis, alveolar septal thickening, cellular desquamation, hyaline membranes, protein-rich exudates in the alveoli, and alveolitis.<sup>35,40,127,140,191</sup> Another common feature of humans and hamsters is moderate to severe diffuse or multifocal bronchointerstitial pneumonia.<sup>24,35,40,127,140,191</sup> In addition, signs of proliferative DAD are present in hamsters, including pulmonary epithelial hyperplasia and hypertrophy, papillary projections into luminal spaces, atypical hyperplastic proliferative type II pneumocytes, and multinucleated cells.<sup>35,40,50,127,140</sup> Furthermore, hamsters exhibit many of the key signs of ALI seen in humans<sup>110</sup> and display similar features of vascular injury, including vascular leakage, alveolar hemorrhage, and vasculitis.<sup>35,40,83,191</sup> Vascular endothelialitis and alveolar fibrin deposition have been reported also.<sup>40,127,140</sup> Although DAD is a hallmark feature of SARS-CoV-2 infection in hamsters, it is not associated with severe morbidity or high mortality, as it is in humans.<sup>32,88</sup>

Inflammatory cell infiltration is another hallmark feature of SARS-CoV-2 infection in both humans and hamsters. Mononuclear cell infiltrates, including macrophages and monocytes, are reported in nearly all parts of the lungs, from the pulmonary interstitium and bronchioles to the alveolar septa and alveolar sacs.<sup>24,35,40,50,83,127,140,143,154</sup> Reports also indicate infiltration of CD3<sup>+</sup> T cells, polymorphonuclear cells, and multinucleated cells into the lungs.<sup>24,143,154</sup> Similar to humans, fibrosis of the lungs occurs during the late stages of infection in hamsters and includes mild, multifocal pleural fibrosis, interstitial fibrosis, and perivascular fibrosis.<sup>40,140</sup>

Hamsters have been used more extensively than other animals to study the pathogenesis of SARS-CoV-2 in the upper respiratory tract. Viral replication kinetics after nasal infection and cellular damage follow a similar timeline as that described for the lungs. Nasal pathology after SARS-CoV-2 infection includes epithelial cell death and desquamation, submucosal infiltration in the nasal turbinates, accumulation of cell debris in the terminal space, and olfactory sensory nerve desquamation.<sup>193</sup> After intranasal infection, viral antigen has been detected in nasal epithelial cells, nasal mucosa, and sensory neurons, suggesting that hamsters might develop anosmia, one of the hallmark symptoms of COVID-19 in humans.<sup>193</sup>

## Mice as Models of SARS-CoV-2–induced Respiratory Disease and Lung Pathology

Mice (*Mus musculus*) are often used to model human disease due to their small size, relatively low cost, ease of genetic manipulation, wide availability of reagents, and ability to control many environmental factors to best replicate human disease. Although SARS-CoV-2 can infect standard inbred mice via endogenous mouse ACE2 (mACE2), viral replication is low and does not result in severe disease as occurs in humans.<sup>1</sup> Many mouse models have been proposed to better reflect the disease and pathology observed in humans, but the discussion here will be limited to 2 main approaches: a transgenic approach (K18-hACE2 mice) and a mouse adaptation approach (SARS-CoV-2–MA10 strain). Both of these models are available to the research community,

either as mice purchased from animal vendors or as viral stocks obtained from the Biodefense and Emerging Infections Research Resources Repository (BEI Resources).<sup>7</sup>

A common and well-characterized transgenic model used to study SARS-CoV-2 is the K18-hACE2 (K18) mouse. First created in response to the 2003 SARS-CoV epidemic, K18 mice express human ACE2 under the control of the human cytokeratin 18 promoter.<sup>112</sup> The S glycoproteins of both SARS-CoV and SARS-CoV-2 have higher binding affinity to human ACE2 than to mouse ACE2 on epithelial cells. Most importantly, human ACE2 is expressed on airway epithelia, a key site of SARS-CoV-2 infection and replication, in the K18 model. Virus is frequently detectable in the brains of K18 mice after infection but does not typically result in signs of neurologic disease.<sup>67,136,189</sup> The presence of virus in the brain of K18 mice likely reflects an overexpression of human ACE2 beyond what is physiologically normal in humans. However, the K18 model includes anosmia, which occurs in both symptomatic and asymptomatic COVID-19 patients.<sup>197</sup> K18 mice may exhibit disease that is more severe and less confined to the respiratory system than that of humans.

The cellular targets of SARS-CoV-2 in the lower respiratory tract of K18 mice are almost exclusively alveolar epithelial cells.<sup>33</sup> Viral titers peak at 4 dpi and localize primarily in type I pneumocytes and, to a lesser extent, type II pneumocytes. By 6 dpi, virus particles are found in both type I and type II pneumocytes. Overall, this pattern of infection differs from that of humans, in which type II pneumocytes are the primary site of infection. The bronchiolar epithelium, including ciliated and nonciliated (club) cells, shows no evidence of infection. Furthermore, the pulmonary endothelial cells of K18 mice are not infected,<sup>33</sup> another difference from the human form of the disease, in which virus is found in both conducting airway epithelia and pulmonary endothelial cells.

More recently, several groups have used virus adaptation to provide better binding of the S glycoprotein of SARS-CoV-2 to mouse ACE2 and allow infection in mice.<sup>51,72,100,122,159,181</sup> The first strain to be published, named SARS-CoV-2-MA (mouse-adapted), was created by using reverse genetics to alter key residues of the S glycoprotein.<sup>51</sup> Serial passage of this virus strain in BALB/c mice yielded a more pathogenic virus, named SARS-CoV-2-MA10 (MA10).<sup>100</sup> Additional mouse-adapted strains have been developed through serial passage with or without the aid of reverse genetics and show different mutations in the S glycoprotein and nonstructural viral proteins.<sup>72,122,159,181</sup> Each of these viral strains results in successful infection of standard inbred mouse strains, severe clinical disease, and pathology mirroring that commonly seen in human patients.<sup>72,100,122,159,181</sup> These characteristics are useful in investigating the pathologic mechanisms of SARS-CoV-2-associated disease and potential therapeutics.

In situ hybridization in MA10 mice revealed selective infection of type II pneumocytes, reflective of the cellular tropism of SARS-CoV-2 in humans, accompanied by a loss of surfactant protein transcripts (*Sftpc* and *Sftpb*) during the peak of viral replication at 2 dpi.<sup>100</sup> In the terminal bronchiolar region, SARS-CoV-2 antigen selectively colocalizes with secretory club cells rather than ciliated epithelial cells. This finding suggests selective infection of club cells, a phenomenon that has not been reported in humans.<sup>100</sup>

Infectious virus has been detected in the lungs of K18 mice as early as 2 d after intranasal inoculation.<sup>136,178,197</sup> Viral RNA in the lung is found primarily in alveolar epithelial cells and, as the infection progresses, expression diminishes in association

with the accumulation of cellular debris and collapsed alveoli.<sup>178</sup> Viral RNA has been detected in nasal turbinates until 8 dpi, with minimal pathology and cellular sloughing in the olfactory epithelium.<sup>67,136,197</sup> At later time points (6 to 7 dpi), infectious virus and viral RNA have both been detected in the brain.<sup>197</sup> In the MA10 model, viral replication in the lung peaks at 1 to 2 dpi and drops below detectable levels by 7 dpi in 10- to 12-wk-old BALB/c and C57BL/6J mice.<sup>100</sup> Viral antigen labeling follows a similar trend, is localized primarily in type II pneumocytes, and is associated with a loss of surfactant protein transcripts. Infection of aged BALB/c mice shows a similar peak in viral replication at 1 to 2 dpi; however, replication levels are maintained throughout the course of the infection.<sup>100,136</sup> This pattern is consistent with the exacerbation of disease severity with age in humans.

General signs of disease for both K18 mice and MA10-infected BALB/c mice include rapid weight loss, lethargy, ruffled fur, hunched posture, and labored breathing.<sup>67,100,136,189</sup> Both models show dose-dependent increases in morbidity and mortality, with many mice reaching euthanasia criteria by 7 dpi.<sup>67,100,178,197</sup> The MA10 model shows variable recovery in the later stages of infection for young adult mice, with some mice recovering and others continuing to lose weight, ultimately resulting in 15% to 20% mortality by 7 dpi. Aged mice inoculated with 10<sup>4</sup> pfu of MA10 progressively lose weight, reflecting severe disease seen in elderly humans.<sup>100</sup> Most studies of SARS-CoV-2 infection in K18 mice report no sex-associated differences in weight loss and mortality, although one study showed significant higher mortality in male mice infected with a low dose of virus.<sup>67</sup> In addition, K18 mice exhibit signs of lymphopenia accompanied by neutrophilia in the systemic circulation, with decreased numbers of B cells, CD4<sup>+</sup> T cells, CD8<sup>+</sup> T cells, and monocytes at 5 dpi.<sup>178</sup> The severity of disease induced by MA10 is dependent on host genetic factors. Infection of C57BL/6J mice with MA10 resulted in less severe disease and no mortality as compared with BALB/c mice.<sup>100</sup> Depending on the goals of the study, this difference may help to achieve a specifically desired level of disease severity. However, in order to reproduce key disease phenotypes of COVID-19 patients, especially in severe cases, MA10 must be used in mouse strains that are relatively more susceptible to infection.

Pulmonary function after SARS-CoV-2 infection has been evaluated in mice. K18 mice display reduced lung compliance after SARS-CoV-2 infection. Results of a treadmill stress test show reduced exercise tolerance of infected mice at 5 dpi.<sup>178</sup> Based on results of mechanical ventilation and forced oscillation tests, abnormal lung parameters, characterized by reduced inspiratory capacity and increased respiratory resistance and elastance, can be detected by 7 dpi. Lastly, broadband forced oscillation maneuvers have revealed elevated tissue damping, elastance and stiffness in the peripheral airway, indicating that the primary site of disease is the lung parenchyma.<sup>178</sup> In MA10-infected mice, whole-body plethysmography revealed increases in enhanced pause (PenH) and midexpiratory flow (EF<sub>50</sub>) and a decrease in the peak expiratory flow rate (R<sub>pef</sub>),<sup>100</sup> indicating impaired pulmonary function.<sup>114</sup> As compared with humans, both models (K18 and MA10) exhibit physiologic lung dysfunction after infection, including low compliance and reduced inspiratory capacity. Due to differences in lung anatomy and physiology between mice and humans, mouse measurements are not entirely accurate, nor as robust, as those of human patients. For example, important markers of physiologic dysfunction, such as arterial oxygen partial pressure, are not easily measured in mice due to their low systemic blood



	Similarities to COVID-19 in humans	Differences from COVID-19 in humans
NHP	<p><b>Clinical Disease</b></p> <ul style="list-style-type: none"> <li>• high interindividual disease variability</li> <li>• most cases are mild to moderate severity</li> <li>• time course of disease</li> <li>• age associated with more severe disease</li> <li>• fever and lethargy</li> <li>• monocytosis, neutrophilia, lymphopenia</li> <li>• elevated markers of systemic inflammation</li> </ul> <p><b>Lung Pathology</b></p> <ul style="list-style-type: none"> <li>• infection of epithelial cells, including airway epithelium and pneumocytes</li> <li>• lung consolidation and hemorrhage</li> <li>• interstitial pneumonia</li> <li>• endotheliitis or vasculitis, microthrombosis</li> <li>• inflammatory infiltrates</li> <li>• fibrosis</li> </ul>	<p><b>Clinical Disease</b></p> <ul style="list-style-type: none"> <li>• severe cases rare</li> <li>• no sex-associated differences</li> <li>• mild weight loss common</li> <li>• coughing, dyspnea, and hypoxemia uncommon</li> <li>• overt coagulopathy rare</li> </ul> <p><b>Lung Pathology</b></p> <ul style="list-style-type: none"> <li>• severe diffuse alveolar damage involving hyaline membranes rare</li> </ul>
Hamsters	<p><b>Clinical Disease</b></p> <ul style="list-style-type: none"> <li>• high interindividual disease variability</li> <li>• lethargy</li> <li>• age and male sex associated with more severe disease</li> <li>• elevated markers of systemic inflammation</li> </ul> <p><b>Lung Pathology</b></p> <ul style="list-style-type: none"> <li>• interstitial pneumonia</li> <li>• acute lung injury and diffuse alveolar damage</li> <li>• lung congestion and edema</li> <li>• vascular injury</li> <li>• inflammatory infiltrates</li> <li>• fibrosis</li> </ul>	<p><b>Clinical Disease</b></p> <ul style="list-style-type: none"> <li>• minimal incubation period</li> <li>• minimal clinical signs of disease</li> </ul> <p><b>Lung Pathology</b></p> <ul style="list-style-type: none"> <li>• pulmonary microthrombi rare</li> </ul>
Mice	<p><b>Clinical Disease</b></p> <ul style="list-style-type: none"> <li>• dyspnea</li> <li>• elevated markers of systemic inflammation</li> <li>• systemic lymphopenia and neutrophilia (K18)</li> <li>• pulmonary coagulopathy (K18)</li> <li>• increased severity with age (MA10)</li> <li>• low pulmonary compliance</li> <li>• impaired respiratory function</li> </ul> <p><b>Lung Pathology</b></p> <ul style="list-style-type: none"> <li>• acute lung injury and diffuse alveolar damage</li> <li>• lung congestion and edema</li> <li>• vasculitis and thrombus formation (K18)</li> <li>• inflammatory infiltrates</li> </ul>	<p><b>Clinical Disease</b></p> <ul style="list-style-type: none"> <li>• no consistent sex-based differences</li> <li>• direct infection of the brain (K18)</li> <li>• rapid decline and death</li> </ul> <p><b>Lung Pathology</b></p> <ul style="list-style-type: none"> <li>• robust type I pneumocyte infection (K18)</li> <li>• lack of viral replication in bronchiolar epithelial cells or pulmonary endothelial cells (K18)</li> <li>• secretory club cell infection (MA10)</li> <li>• no infection of ciliated bronchiolar epithelial cells (MA10)</li> </ul>

**Figure 2.** Similarities to and differences from SARS-CoV-2-induced respiratory disease and pathology in animal models compared with humans. K18, K18-hACE2 transgenic mice; MA10, MA10 mice infected with mouse adapted SARS-CoV-2.

volume. Despite these limitations, both mouse models show evidence of lung dysfunction, as well as overt signs of dyspnea.

Similar to COVID-19 in humans, SARS-CoV-2 infection in both the K18 and MA10 models is associated with the upregulation of proinflammatory cytokines and chemokines. TNF $\alpha$ , IL6, GM-CSF, CCL2, CCL7, CXCL10, and keratinocyte chemoattractant (an ortholog of human IL8) are all elevated in K18 mouse serum after infection;<sup>67,189</sup> another study reported upregulation of IL10.<sup>131</sup> The serum of aged MA10-infected mice has elevated levels of IL6, IFN $\gamma$ , G-CSF, and CCL2. In addition, plasma levels of D-dimers are elevated at 2 and 4 dpi, followed by elevation of bicarbonate anion concentration, hematocrit (Hct), hemoglobin (Hgb), and prothrombin time at 7 dpi.<sup>178</sup> These results are consistent with the hypercapnia and coagulopathy seen in COVID-19 patients. Taken together, results of blood analysis from both models shares many features with results seen in COVID-19 patients.

Due to the small size of mice, BALF collection is not commonly performed after SARS-CoV-2 infection; however, one study in K18 mice revealed an increase in CD45<sup>+</sup> cells at 2 dpi, a peak in monocyte numbers at 4 dpi, and an increase in neutrophil and dendritic cell numbers through 7 dpi.<sup>178</sup> Instead,

protein evaluation of lungs collected at necropsy has been performed in both K18 and MA10 models. Lung homogenates of infected K18 mice display increases in IFN $\beta$ , IFN $\gamma$ , TNF- $\alpha$ , G-CSF, IL1 $\beta$ , IL6, IL10, CXCL1, CXCL9, CXCL10, CCL2, CCL3, CCL4, CCL5, and CCL12.<sup>67,136,178</sup> Increases in transcripts associated with hypoxia, including *Sgp11*, *Retnla*, *Cxcl12*, and *Hif1a*, have been reported also.<sup>67</sup> Lung homogenates of aged MA10 mice show increases in TNF $\alpha$ , IL1 $\alpha$ , IL1 $\beta$ , G-CSF, IL5, IL6, IL10, and CCL2.<sup>100</sup> Overall, both the K18 and MA10 mouse models recapitulate many of the same proinflammatory signals that are characteristic of ALI in humans.

Compared with NHP, the lung pathology of mice infected with SARS-CoV-2 tends to be more severe. At necropsy, as much as 80% of the lungs of K18 mice is grossly affected.<sup>189</sup> In the MA10 model, lungs tend to be firm, red and heavy.<sup>100</sup> Based on scoring of gross lung discoloration, aged mice show maximal discoloration scores on 4 to 5 dpi, indicating congestion, edema, and DAD.<sup>100</sup>

As discussed above, ALI is a key feature of human SARS-CoV-2 infection that can result in respiratory failure and ARDS. Features of ALI include rapid onset (within 24 h of exposure), histologic evidence of tissue injury, alteration of the alveolar-

capillary barrier, presence of an inflammatory response, and evidence of pulmonary physiologic dysfunction.<sup>110</sup> Furthermore, the pathologic hallmark of ALI in humans is DAD.<sup>110</sup> The correlation of ALI and DAD with death in severe COVID-19 makes this feature of SARS-CoV-2 infection crucial in modeling the disease in mice. Accordingly, the American Thoracic Society has devised a scoring system to determine the level of ALI in animals based on the presence of neutrophils in alveolar and interstitial spaces, the formation of hyaline membranes, alveolar septal thickening, and proteinaceous debris in air spaces. In addition, a semiquantitative ordinal scale of 0, 1, or 2 based on all examined fields of lung tissue summarizes the extent of ALI in terms of histologic evidence.<sup>110</sup> Both approaches document an inflammatory response and changes in pulmonary function as features of ALI in mice.

DAD is common after infection in both K18 mice and MA10 mice, consistent with many of the features observed in humans. As with ALI, a scoring system created initially to evaluate the extent of DAD in mice infected with respiratory syncytial virus has been adapted to evaluate lung pathology in MA10-infected mice.<sup>148</sup> This semiquantitative ordinal scale scoring system ranging from 1 to 4 assesses the presence of cellular degeneration, sloughing, and necrosis, alveolar hemorrhage, cellular infiltrates, and hyaline membrane formation. In MA10 mice, DAD and ALI scores increase starting at 2 dpi and remain high throughout acute infection.<sup>100</sup> Pulmonary histopathology is characterized by epithelial cell sloughing, degeneration, or attenuation, segmental epithelial denudation, accumulation of leukocytes, fibrin, plasma proteins, and cellular debris in the airway lumen, and variable congestion and edema.<sup>90</sup> However, the most severe damage occurs in the alveolar region, with mild hypercellular thickening of alveolar septa due to immune cell infiltration, pneumocyte necrosis, capillary congestion, and exudation of proteinaceous fluid and fibrin with occasional hyaline membranes.<sup>100</sup> Mice infected with MA10 have many features of severe disease and develop DAD, especially in association with hyaline membranes, which are not frequent in infected mice.<sup>90,110</sup> In BALB/c mice, the severity of DAD scores correlates with viral lung titers at the height of acute disease (3 to 5 dpi).<sup>100</sup>

Another scoring system has been developed to quantify the pathology seen in K18 mice. This system generates a composite score based on the area of lung affected and 8 histologic markers, including perivascular inflammation, epithelial necrosis of bronchi and bronchioles, bronchial and bronchiolar inflammation, intraluminal debris in bronchi and bronchioles, alveolar inflammation, alveolar necrosis, fibrin deposition, and hyperplasia of type II pneumocytes.<sup>136</sup> However, the use of this scoring system revealed that the pathology seen in K18 mice was low in comparison to viral presence in the lungs,<sup>136</sup> reflecting the need for standardization to better compare the histopathology of K18 mice and humans.

After infection, K18 mice develop interstitial infiltration of macrophages, neutrophils, and CD3<sup>+</sup> T cells.<sup>67,197</sup> Alveolar septal thickening occurs during infection, with Ly6G<sup>+</sup> neutrophils and mononuclear cells occupying alveolar and interstitial spaces at 7 dpi.<sup>178</sup> In addition, increases occur in numbers of Ly6C<sup>+</sup> monocytes, CD11b<sup>+</sup>CD11c<sup>+</sup> dendritic cells, NK cells, CD4<sup>+</sup> T cells, CD8<sup>+</sup> T cells, and CD44<sup>+</sup>CD8<sup>+</sup> T cells. These inflammatory infiltrates are similar to those seen in COVID-19 patients. MA10 infection also results in inflammatory infiltrate in the alveolar space. Although present, variable peribronchiolar and perivascular lymphocytic inflammation is not considered a key pathologic feature of ALI and thus is not scored in acute

MA10 infection.<sup>100</sup> As indicated by the increase in inflammatory cytokines, infection with MA10 results in a proinflammatory response, but the specific inflammatory cells involved require better characterization.

## Conclusions

Although NHP, hamsters, and mice replicate many features of SARS-CoV-2-induced respiratory disease and pathology seen in humans, each animal model has limitations. When designing SARS-CoV-2 studies that use animals, an important consideration for maximizing the translational potential of the study is to recognize the model's similarities to and differences from humans (Figure 2). Because no single animal model captures all features of COVID-19 infection in humans, the best species to use will depend on the particular type of study. Practical factors, including animal size, housing, cost, and availability of applicable reagents, should also be considered. For example, although NHP may be better suited for evaluating the immunogenicity and efficacy of a potential mucosal vaccine that prevents infection in the upper respiratory tract, hamsters might be better suited to the evaluation of a potential treatment designed to mitigate the development of severe respiratory disease. Alternatively, the large arsenal of immunologic reagents and relative ease and availability of genetic modification make mice a valuable model for detailed mechanistic studies evaluating the pathogenesis and immune response of SARS-CoV-2 infection. Appropriate use of animal models of SARS-CoV-2-induced respiratory disease will promote increased understanding of SARS-CoV-2 pathogenesis and the development of additional preventatives and therapies.

## Acknowledgments

This work was supported by NIH grant K01OD026529 (to VKB).

## References

1. Abdel-Moneim AS, Abdelwhab EM. 2020. Evidence for SARS-CoV-2 infection of animal hosts. *Pathogens* 9:529. <https://doi.org/10.3390/pathogens9070529>.
2. Ackermann M, Verleden SE, Kuehnel M, Haverich A, Welte T, Laenger F, Vanstapel A, Werlein C, Stark H, Tzankov A, Li WW, Li VW, Mentzer SJ, Jonigk D. 2020. Pulmonary vascular endothelialitis, thrombosis, and angiogenesis in COVID-19. *N Engl J Med* 383:120–128. <https://doi.org/10.1056/NEJMoa2015432>.
3. Ahn JH, Kim J, Hong SP, Choi SY, Yang MJ, Ju YS, Kim YT, Kim HM, Rahman MT, Chung MK, Hong SD, Bae H, Lee CS, Koh GY. 2021. Nasal ciliated cells are primary targets for SARS-CoV-2 replication in early stage of COVID-19. *J Clin Invest* 131:e148517. <https://doi.org/10.1172/JCI148517>.
4. Aid M, Busman-Sahay K, Vidal SJ, Maliga Z, Bondoc S, Starke C, Terry M, Jacobson CA, Wrijil L, Ducat S, Brook OR, Miller AD, Porto M, Pellegrini KL, Pino M, Hoang TN, Chandrashekar A, Patel S, Stephenson K, Bosinger SE, Andersen H, Lewis MG, Hecht JL, Sorger PK, Martinot AJ, Estes JD, Barouch DH. 2020. Vascular disease and thrombosis in SARS-CoV-2-infected rhesus macaques. *Cell* 183:1354–1366.e13. <https://doi.org/10.1016/j.cell.2020.10.005>.
5. Albrecht L, Bishop E, Jay B, Lafoux B, Minoves M, Passaes C. 2021. COVID-19 research: Lessons from nonhuman primate models. *Vaccines* 9:886. <https://doi.org/10.3390/vaccines9080886>.
6. ARDS Definition Task Force. 2012. Acute respiratory distress syndrome: The Berlin definition. *JAMA* 307:2526–2533. <https://doi.org/10.1001/jama.2012.5669>.
7. Baker R, Peacock S. 2008. BEI resources: Supporting antiviral research. *Antiviral Res* 80:102–106. <https://doi.org/10.1016/j.antiviral.2008.07.003>.
8. Ball L, Robba C, Herrmann J, Gerard SE, Xin Y, Mandelli M, Battaglini D, Brunetti I, Minetti G, Seitun S, Bovio G, Vena A,

- Giacobbe DR, Bassetti M, Rocco PRM, Cereda M, Rizi RR, Castellan L, Patroniti N, Pelosi P; Collaborators of the GECOVID Group. 2021. Lung distribution of gas and blood volume in critically ill COVID-19 patients: A quantitative dual-energy computed tomography study. *Crit Care* 25:214. <https://doi.org/10.1186/s13054-021-03610-9>.
9. Ball L, Robba C, Maiello L, Herrmann J, Gerard SE, Xin Y, Battaglini D, Brunetti I, Minetti G, Seitun S, Vena A, Giacobbe DR, Bassetti M, Rocco PRM, Cereda M, Castellan L, Patroniti N, Pelosi P; GECOVID (GEnoa COVID-19) Group. 2021. Computed tomography assessment of PEEP-induced alveolar recruitment in patients with severe COVID-19 pneumonia. *Crit Care* 25:81. <https://doi.org/10.1186/s13054-021-03477-w>.
  10. Ball L, Silva PL, Giacobbe DR, Bassetti M, Zubieta-Calleja GR, Rocco PRM, Pelosi P. 2022. Understanding the pathophysiology of typical acute respiratory distress syndrome and severe COVID-19. *Expert Rev Respir Med* 16:437–446. <https://doi.org/10.1080/17476348.2022.2057300>.
  11. Bao C, Liu X, Zhang H, Li Y, Liu J. 2020. Coronavirus disease 2019 (COVID-19) CT findings: A systematic review and meta-analysis. *J Am Coll Radiol* 17:701–709. <https://doi.org/10.1016/j.jacr.2020.03.006>.
  12. Barisione E, Grillo F, Ball L, Bianchi R, Grosso M, Morbini P, Pelosi P, Patroniti NA, Lucia AD, Orenzo G, Gratarola A, Verda M, Cittadini G, Mastracci L, Fiocca R. 2021. Fibrotic progression and radiologic correlation in matched lung samples from COVID-19 postmortems. *Virchows Arch* 478:471–485. <https://doi.org/10.1007/s00428-020-02934-1>.
  13. Barnes BJ, Adrover JM, Baxter-Stoltzfus A, Borczuk A, Cools-Lartigue J, Crawford JM, Daßler-Plenker J, Guerci P, Huynh C, Knight JS, Loda M, Looney MR, McAllister F, Rayes R, Renaud S, Rousseau S, Salvatore S, Schwartz RE, Spicer JD, Weber A, Zuo Y, Egeblad M. 2020. Targeting potential drivers of COVID-19: Neutrophil extracellular traps. *J Exp Med* 217:e20200652. <https://doi.org/10.1084/jem.20200652>.
  14. Baron A, Hachem M, Nhieu JTV, Botterel F, Fourati S, Carreaux G, Prost ND, Maitre B, Mekontso-Dessap A, Schlemmer F. 2021. Bronchoalveolar lavage in patients with COVID-19 with invasive mechanical ventilation for acute respiratory distress syndrome. *Ann Am Thorac Soc* 18:723–726. <https://doi.org/10.1513/AnnalsATS.202007-868RL>.
  15. Barton LM, Duval EJ, Stroberg E, Ghosh S, Mukhopadhyay S. 2020. COVID-19 autopsies: Oklahoma, USA. *Am J Clin Pathol* 153:725–733. <https://doi.org/10.1093/ajcp/aqaa062>.
  16. Berlin DA, Gulick RM, Martinez FJ. 2020. Severe COVID-19. *N Engl J Med* 383:2451–2460. <https://doi.org/10.1056/NEJM-cp2009575>.
  17. Bharat A, Querrey M, Markov NS, Kim S, Kurihara C, Garza-Castillon R, Manerikar A, Shilatifard A, Tomic R, Politanska Y, Abdala-Valencia H, Yeldandi AV, Lomasney JW, Misharin AV, Budinger GRS. 2020. Lung transplantation for patients with severe COVID-19. *Sci Transl Med* 12:eabe4282. <https://doi.org/10.1126/scitranslmed.abe4282>.
  18. Bixler SL, Stefan CP, Jay AN, Rossi FD, Ricks KM, Shoemaker CJ, Moreau AM, Zeng X, Hooper JW, Dyer DN, Frick OM, Koehler JW, Kearney BJ, DiPinto N, Liu J, Tostenson SD, Clements TL, Smith JM, Johnson JA, Berrier KL, Esham HL, Delp KL, Coyne SR, Bloomfield HA, Kuehnert PA, Akers K, Gibson KM, Minogue TD, Nalca A, Pitt MLM. 2022. Exposure route influences disease severity in the COVID-19 cynomolgus macaque model. *Viruses* 14:1013. <https://doi.org/10.3390/v14051013>.
  19. Blair RV, Vaccari M, Doyle-Meyers LA, Roy CJ, Russell-Lodrigue K, Fahlberg M, Monjure CJ, Beddingfield B, Plante KS, Plante JA, Weaver SC, Qin X, Midkiff CC, Lehmicke G, Golden N, Threeton B, Penney T, Allers C, Barnes MB, Pattison M, Datta PK, Maness NJ, Birnbaum A, Fischer T, Bohm RP, Rappaport J. 2021. Acute respiratory distress in aged, SARS-CoV-2-infected African green monkeys but not rhesus macaques. *Am J Pathol* 191:274–282. <https://doi.org/10.1016/j.ajpath.2020.10.016>.
  20. Borczuk AC, Salvatore SP, Seshan SV, Patel SS, Bussel JB, Mostyka M, Elsoukary S, He B, Vecchio CD, Fortarezza F, Pezzuto F, Navalesi P, Crisanti A, Fowkes ME, Bryce CH, Calabrese F, Beasley MB. 2020. COVID-19 pulmonary pathology: A multi-institutional autopsy cohort from Italy and New York City. *Mod Pathol* 33:2156–2168. <https://doi.org/10.1038/s41379-020-00661-1>.
  21. Bösmüller H, Matter M, Fend F, Tzankov A. 2021. The pulmonary pathology of COVID-19. *Virchows Arch* 478:137–150. <https://doi.org/10.1007/s00428-021-03053-1>.
  22. Bösmüller H, Traxler S, Bitzer M, Häberle H, Raiser W, Nann D, Frauenfeld L, Vogelsberg A, Klingel K, Fend F. 2020. The evolution of pulmonary pathology in fatal COVID-19 disease: An autopsy study with clinical correlation. *Virchows Arch* 477:349–357. <https://doi.org/10.1007/s00428-020-02881-x>.
  23. Böszörményi KP, Stammes MA, Fagrouch ZC, Kiemenyi-Kayere G, Niphuis H, Mortier D, van Driel N, Nieuwenhuis I, Vervenne RAW, Haakma T, Ouwerling B, Adema D, Acar RF, Zuiderwijk-Sick E, Meijer L, Mooij P, Remarque EJ, Oostermeijer H, Koopman G, Hoste ACR, Sastre P, Haagmans BL, Bontrop RE, Langermans JAM, Bogers WM, Kondova I, Verschoor EJ, Verstrepen BE. 2021. The postacute phase of SARS-CoV-2 infection in 2 macaque species is associated with signs of ongoing virus replication and pathology in pulmonary and extrapulmonary tissues. *Viruses* 13:1673. <https://doi.org/10.3390/v13081673>.
  24. Boudewijns R, Thibaut HJ, Kaptein SJF, Li R, Vergote V, Seldeslachts L, Weyenbergh JV, Keyzer CD, Bervoets L, Sharma S, Liesenborghs L, Ma J, Jansen S, Van Looveren D, Vercrusse T, Wang X, Jochmans D, Martens E, Roose K, De Vlieger D, Schepens B, Van Buyten T, Jacobs S, Liu Y, Marti-Carreras J, Vanmechelen B, Wawina-Bokalanga T, Delang L, Rocha-Pereira J, Coelmont L, Chiu W, Leyssen P, Heylen E, Schols D, Wang L, Close L, Matthijnsens J, Van Ranst M, Compernelle V, Schramm G, Van Laere K, Saelens X, Callewaert N, Opendakker G, Maes P, Weyand B, Cawthorne C, Vande Velde G, Wang Z, Neyts J, Dallmeier K. 2020. STAT2 signaling restricts viral dissemination but drives severe pneumonia in SARS-CoV-2-infected hamsters. *Nat Commun* 11:5838. <https://doi.org/10.1038/s41467-020-19684-y>.
  25. Bradley BT, Maioli H, Johnston R, Chaudhry I, Fink SL, Xu H, Najafian B, Deutsch G, Lacy JM, Williams T, Yarid N, Marshall DA. 2020. Histopathology and ultrastructural findings of fatal COVID-19 infections in Washington State: A case series. *Lancet* 396:320–332. [https://doi.org/10.1016/S0140-6736\(20\)31305-2](https://doi.org/10.1016/S0140-6736(20)31305-2).
  26. Braxton AM, Creisher PS, Ruiz-Bedoya CA, Mulka KR, Dhakal S, Ordonez AA, Beck SE, Jain SK, Villano JS. 2021. Hamsters as a model of severe acute respiratory syndrome coronavirus 2. *Comp Med* 71:398–410. <https://doi.org/10.30802/AALAS-CM-21-000036>.
  27. Brocato RL, Principe LM, Kim RK, Zeng X, Williams JA, Liu Y, Li R, Smith JM, Golden JW, Gangemi D, Youssef S, Wang Z, Glanville J, Hooper JW. 2020. Disruption of adaptive immunity enhances disease in SARS-CoV-2-infected Syrian hamsters. *J Virol* 94:e01683-e20. <https://doi.org/10.1128/JVI.01683-20>.
  28. Budinger GRS, Misharin AV, Ridge KM, Singer BD, Wunderink RG. 2021. Distinctive features of severe SARS-CoV-2 pneumonia. *J Clin Invest* 131:e149412. <https://doi.org/10.1172/JCI149412>.
  29. Calabrese F, Pezzuto F, Fortarezza F, Hofman P, Kern I, Panizo A, von der Thüsen J, Timofeev S, Gorkiewicz G, Lunardi F. 2020. Pulmonary pathology and COVID-19: Lessons from autopsy. The experience of European Pulmonary Pathologists. *Virchows Arch* 477:359–372. <https://doi.org/10.1007/s00428-020-02886-6>.
  30. Cantley RL, Hrycaj S, Konopka K, Chan MP, Huang T, Pantanowitz L. 2021. Cytologic findings in effusions from patients with SARS-CoV-2 infection. *J Am Soc Cytopathol* 10:261–269. <https://doi.org/10.1016/j.jasc.2021.01.003>.
  31. Caravita S, Baratto C, Marco FD, Calabrese A, Balestrieri G, Russo F, Faini A, Soranna D, Perego GB, Badano LP, Grazioli L, Lorini FL, Parati G, Senni M. 2020. Haemodynamic characteristics of COVID-19 patients with acute respiratory distress syndrome requiring mechanical ventilation. An invasive assessment using right heart catheterization. *Eur J Heart Fail* 22:2228–2237. <https://doi.org/10.1002/ejhf.2058>.



32. Cardinal-Fernández P, Bajwa EK, Dominguez-Calvo A, Menéndez JM, Papazian L, Thompson BT. 2016. The presence of diffuse alveolar damage on open lung biopsy is associated with mortality in patients with acute respiratory distress. *Chest* 149:1155–1164. <https://doi.org/10.1016/j.chest.2016.02.635>.
33. Carosino M, Kenney D, O'Connell AK, Montanaro P, Tseng AE, Gertje HP, Grosz KA, Ericsson M, Huber BR, Kurnick SA, Subramaniam S, Kirkland TA, Walker JR, Francis KP, Klose AD, Paragas N, Bosmann M, Saeed M, Balasuriya UBR, Douam F, Crossland NA. 2022. Fatal neurodissemination and SARS-CoV-2 tropism in K18-hACE2 mice is only partially dependent on hACE2 expression. *Viruses* 14:535. <https://doi.org/10.3390/v14030535>.
34. Carsana L, Sonzogni A, Nasr A, Rossi RS, Pellegrinelli A, Zerbi P, Rech R, Colombo R, Antinori S, Corbellino M, Galli M, Catena E, Tosoni A, Gianatti A, Nebuloni M. 2020. Pulmonary postmortem findings in a series of COVID-19 cases from northern Italy: A 2-center descriptive study. *Lancet Infect Dis* 20:1135–1140. [https://doi.org/10.1016/S1473-3099\(20\)30434-5](https://doi.org/10.1016/S1473-3099(20)30434-5).
35. Chan JF-W, Zhang AJ, Yuan S, Poon VK-M, Chan CC-S, Lee AC-Y, Chan W-M, Fan Z, Tsoi H-W, Wen L, Liang R, Cao J, Chen Y, Tang K, Luo C, Cai JP, Kok KH, Chu H, Chan KH, Sridhar S, Chen Z, Chen H, To KK, Yuen KY. 2020. Simulation of the clinical and pathological manifestations of Coronavirus Disease 2019 (COVID-19) in golden Syrian hamster model: Implications for disease pathogenesis and transmissibility. *Clin Infect Dis* 71:2428–2446. <https://doi.org/10.1093/cid/ciaa325>.
36. Chandrashekar A, Liu J, Martinot AJ, McMahan K, Mercado NB, Peter L, Tostanoski LH, Yu J, Maliga Z, Nekorchuk M, Busman-Sahay K, Terry M, Wrijil LM, Ducat S, Martinez DR, Atyeo C, Fischinger S, Burke JS, Slein MD, Pessaint L, Van Ry A, Greenhouse J, Taylor T, Blade K, Cook A, Finneyfrock B, Brown R, Teow E, Velasco J, Zahn R, Wegmann F, Abbink P, Bondzie EA, Dagotto G, Gebre MS, He X, Jacob-Dolan C, Kordana N, Li Z, Lifton MA, Mahrokhian SH, Maxfield LF, Nityanandam R, Nkolola JP, Schmidt AG, Miller AD, Baric RS, Alter G, Sorger PK, Estes JD, Andersen H, Lewis MG, Barouch DH. 2020. SARS-CoV-2 infection protects against rechallenge in rhesus macaques. *Science* 369:812–817. <https://doi.org/10.1126/science.abc4776>.
37. Chang MC, Hild S, Grieder F. 2021. Nonhuman primate models for SARS-CoV-2 research: Consider alternatives to macaques. *Lab Anim (NY)* 50:113–114. <https://doi.org/10.1038/s41684-021-00755-6>.
38. Chen G, Wu D, Guo W, Cao Y, Huang D, Wang H, Wang T, Zhang X, Chen H, Yu H, Zhang X, Zhang M, Wu S, Song J, Chen T, Han M, Li S, Luo X, Zhao J, Ning Q. 2020. Clinical and immunologic features in severe and moderate coronavirus disease 2019. *J Clin Invest* 130:2620–2629. <https://doi.org/10.1172/JCI137244>.
39. Chen N, Zhou M, Dong X, Qu J, Gong F, Han Y, Qiu Y, Wang J, Liu Y, Wei Y, Xia J, Yu T, Zhang X, Zhang L. 2020. Epidemiological and clinical characteristics of 99 cases of 2019 novel coronavirus pneumonia in Wuhan, China: A descriptive study. *Lancet* 395:507–513. [https://doi.org/10.1016/S0140-6736\(20\)30211-7](https://doi.org/10.1016/S0140-6736(20)30211-7).
40. Choudhary S, Kanevsky I, Yildiz S, Sellers RS, Swanson KA, Franks T, Rathnasinghe R, Munoz-Moreno R, Jangra S, Gonzalez O, Meade P, Coskran T, Qian J, Lanz TA, Johnson JG, Tierney CA, Smith JD, Tompkins K, Illenberger A, Corts P, Ciolino T, Dormitzer PR, Dick EJ Jr, Shivanna V, Hall-Ursone S, Cole J, Kaushal D, Fontenot JA, Martinez-Romero C, McMahon M, Krammer F, Schotsaert M, García-Sastre A. 2022. Modeling SARS-CoV-2: comparative pathology in rhesus macaque and golden Syrian hamster models. *Toxicol Pathol* 50:280–293. <https://doi.org/10.1177/01926233211072767>.
41. Chua RL, Lukassen S, Trump S, Hennig BP, Wendisch D, Pott F, Debnath O, Thürmann L, Kurth F, Völker MT, Kazmierski J, Timmermann B, Twardziok S, Schneider S, Machleidt F, Müller-Redetzky H, Maier M, Krannich A, Schmidt S, Balzer F, Liebig J, Loske J, Suttorp N, Eils J, Ishaque N, Liebert UG, von Kalle C, Hocke A, Witzenth M, Goffinet C, Drosten C, Laudi S, Lehmann I, Conrad C, Sander LE, Eils R. 2020. COVID-19 severity correlates with airway epithelium-immune cell interactions identified by single-cell analysis. *Nat Biotechnol* 38:970–979. <https://doi.org/10.1038/s41587-020-0602-4>.
42. Clancy CS, Shaia C, Munster V, de Wit E, Hawman D, Okumura A, Feldmann H, Saturday G, Scott D. 2022. Histologic pulmonary lesions of SARS-CoV-2 in 4 nonhuman primate species: An institutional comparative review. *Vet Pathol* 59:673–680. <https://doi.org/10.1177/03009858211067468>.
43. Cleary SJ, Pitchford SC, Amison RT, Carrington R, Cabrera CLR, Magnen M, Looney MR, Gray E, Page CP. 2020. Animal models of mechanisms of SARS-CoV-2 infection and COVID-19 pathology. *Br J Pharmacol* 177:4851–4865. <https://doi.org/10.1111/bph.15143>.
44. Cross RW, Agans KN, Prasad AN, Borisevich V, Woolsey C, Deer DJ, Dobias NS, Geisbert JB, Fenton KA, Geisbert TW. 2020. Intranasal exposure of African green monkeys to SARS-CoV-2 results in acute phase pneumonia with shedding and lung injury still present in the early convalescence phase. *Virol J* 17:125. <https://doi.org/10.1186/s12985-020-01396-w>.
45. Daamen AR, Bachali P, Owen KA, Kingsmore KM, Hubbard EL, Labonte AC, Robl R, Shrotri S, Grammer AC, Lipsky PE. 2021. Comprehensive transcriptomic analysis of COVID-19 blood, lung, and airway. *Sci Rep* 11:7052. <https://doi.org/10.1038/s41598-021-86002-x>.
46. Dabisch PA, Biryukov J, Beck K, Boydston JA, Sanjak JS, Herzog A, Green B, Williams G, Yeager J, Bohannon JK, Holland B, Miller D, Reese AL, Freeburger D, Miller S, Jenkins T, Rippeon S, Miller J, Clarke D, Manan E, Patty A, Rhodes K, Sweeney T, Winpigler M, Price O, Rodriguez J, Altamura LA, Zimmerman H, Hail AS, Wahl V, Hevey M. 2021. Seroconversion and fever are dose-dependent in a nonhuman primate model of inhalational COVID-19. *PLoS Pathog* 17:e1009865. <https://doi.org/10.1371/journal.ppat.1009865>.
47. Delorey TM, Ziegler CGK, Heimberg G, Normand R, Yang Y, Segerstolpe Å, Abbondanza D, Fleming SJ, Subramanian A, Montoro DT, Jagadeesh KA, Dey KK, Sen P, Slyper M, Pita-Juárez YH, Phillips D, Biermann J, Bloom-Ackermann Z, Barkas N, Ganna A, Gomez J, Melms JC, Katsyiv I, Normandin E, Naderi P, Popov YV, Raju SS, Niezen S, Tsai LT, Siddle KJ, Sud M, Tran VM, Vellarikkal SK, Wang Y, Amir-Zilberstein L, Atri DS, Beechem J, Brook OR, Chen J, Divakar P, Dorceux P, Engreitz JM, Essene A, Fitzgerald DM, Profp R, Gazal S, Gould J, Grzyb J, Harvey T, Hecht J, Hether T, Jané-Valbuena J, Leney-Greene M, Ma H, McCabe C, McLoughlin DE, Miller EM, Muus C, Niemi M, Padera R, Pan L, Pant D, Pe'er C, Pffiffer-Borges J, Pinto CJ, Plaisted J, Reeves J, Ross M, Rudy M, Rueckert EH, Siciliano M, Sturm A, Todres E, Waghay A, Warren S, Zhang S, Zollinger DR, Cosimi L, Gupta RM, Hachohen N, Hibshoosh H, Hilde W, Price AL, Rajagopal J, Tata PR, Riedel S, Szabo G, Tickle TL, Ellinor PT, Hung D, Sabeti PC, Novak R, Rogers R, Ingber DE, Jiang ZG, Juric D, Babadi M, Farhi SL, Izar B, Stone JR, Vlachos IS, Solomon IH, Ashenberg O, Porter CBM, Li B, Shalek AK, Villani AC, Rozenblatt-Rosen O, Regev A. 2021. COVID-19 tissue atlases reveal SARS-CoV-2 pathology and cellular targets. *Nature* 595:107–113. <https://doi.org/10.1038/s41586-021-03570-8>.
48. Deng W, Bao L, Liu J, Xiao C, Liu J, Xue J, Lv Q, Qi F, Gao H, Yu P, Xu Y, Qu Y, Li F, Xiang Z, Yu H, Gong S, Liu M, Wang G, Wang S, Song Z, Liu Y, Zhao W, Han Y, Zhao L, Liu X, Wei Q, Qin C. 2020. Primary exposure to SARS-CoV-2 protects against reinfection in rhesus macaques. *Science* 369:818–823. <https://doi.org/10.1126/science.abc5343>.
49. Desai N, Neyaz A, Szabolcs A, Shih AR, Chen JH, Thapar V, Nieman LT, Solovyov A, Mehta A, Lieb DJ, Kulkarni AS, Jaicks C, Xu KH, Raabe MJ, Pinto CJ, Juric D, Chebib I, Colvin RB, Kim AY, Monroe R, Warren SE, Danaher P, Reeves JW, Gong J, Rueckert EH, Greenbaum BD, Hachohen N, Lagana SM, Rivera MN, Sholl LM, Stone JR, Ting DT, Deshpande V. 2020. Temporal and spatial heterogeneity of host response to SARS-CoV-2 pulmonary infection. *Nat Commun* 11:6319. <https://doi.org/10.1038/s41467-020-20139-7>.
50. Dhakal S, Ruiz-Bedoya CA, Zhou R, Creisher PS, Villano JS, Littlefield K, Castillo JR, Marinho P, Jedlicka AE, Ordonez AA, Bahr M, Majewska N, Betenbaugh MJ, Flavahan K, Mueller ARL, Looney MM, Quijada D, Mota F, Beck SE, Brockhurst J, Braxton AM, Castell N, Stover M, D'Alessio FR, Metcalf Pate KA, Karakousis PC, Mankowski JL, Pekosz A, Jain SK, Klein SL; Johns Hopkins COVID-19 Hamster Study Group. 2021. Sex

- differences in lung imaging and SARS-CoV-2 antibody responses in a COVID-19 golden Syrian hamster model. *MBio* 12:e00974-21. <https://doi.org/10.1128/mBio.00974-21>.
51. Dinnon KH, Leist SR, Schäfer A, Edwards CE, Martinez DR, Montgomery SA, West A, Yount BL, Hou YJ, Adams LE, Gully KL, Brown AJ, Huang E, Bryant MD, Choong IC, Glenn JS, Gralinski LE, Sheahan TP, Baric RS. 2020. A mouse-adapted model of SARS-CoV-2 to test COVID-19 countermeasures. *Nature* 586:560–566. <https://doi.org/10.1038/s41586-020-2708-8>.
  52. Doerschug KC, Schmidt GA. 2022. Pulmonary aspects of COVID-19. *Annu Rev Med* 73:81–93. <https://doi.org/10.1146/annurev-med-042220-014817>.
  53. Dong E, Du H, Gardner L. 2020. An interactive web-based dashboard to track COVID-19 in real time. *Lancet Infect Dis* 20:533–534. [https://doi.org/10.1016/S1473-3099\(20\)30120-1](https://doi.org/10.1016/S1473-3099(20)30120-1).
  54. Drake TM, Docherty AB, Harrison EM, Quint JK, Adamali H, Agnew S, Babu S, Barber CM, Barratt S, Bendstrup E, Bianchi S, Villegas DC, Chaudhuri N, Chua F, Coker R, Chang W, Crawshaw A, Crowley LE, Dosanjh D, Fiddler CA, Forrest IA, George PM, Gibbons MA, Groom K, Haney S, Hart SP, Heiden E, Henry M, Ho LP, Hoyles RK, Hutchinson J, Hurley K, Jones M, Jones S, Kokosi M, Kreuter M, MacKay LS, Mahendran S, Margaritopoulos G, Molina-Molina M, Molyneaux PL, O'Brien A, O'Reilly K, Packham A, Parfrey H, Poletti V, Porter JC, Renzoni E, Rivera-Ortega P, Russell AM, Saini G, Spencer LG, Stella GM, Stone H, Sturney S, Thickett D, Thillai M, Wallis T, Ward K, Wells AU, West A, Wickremasinghe M, Woodhead F, Hearson G, Howard L, Baillie JK, Openshaw PJM, Semple MG, Stewart I, Jenkins RG; ISARIC4C Investigators. 2020. Outcome of hospitalization for COVID-19 in patients with interstitial lung disease. An international multicenter study. *Am J Respir Crit Care Med* 202:1656–1665. <https://doi.org/10.1164/rccm.202007-2794OC>.
  55. Ehaideb SN, Abdullah ML, Abuyassin B, Bouchama A. 2020. Evidence of a wide gap between COVID-19 in humans and animal models: A systematic review. *Crit Care* 24:594. <https://doi.org/10.1186/s13054-020-03304-8>.
  56. Evert K, Dienemann T, Brochhausen C, Lunz D, Lubnow M, Ritzka M, Keil F, Trummer M, Scheiter A, Salzberger B, Reischl U, Boor P, Gessner A, Jantsch J, Calvisi DF, Evert M, Schmidt B, Simon M. 2021. Autopsy findings after long-term treatment of COVID-19 patients with microbiological correlation. *Virchows Arch* 479:97–108. <https://doi.org/10.1007/s00428-020-03014-0>.
  57. Evrard B, Goudelin M, Montmagnon N, Fedou A-L, Lafon T, Vignon P. 2020. Cardiovascular phenotypes in ventilated patients with COVID-19 acute respiratory distress syndrome. *Crit Care* 24:236. <https://doi.org/10.1186/s13054-020-02958-8>.
  58. Fahlberg MD, Blair RV, Doyle-Meyers LA, Midkiff CC, Zenere G, Russell-Lodrigue KE, Monjure CJ, Haupt EH, Penney TP, Lehmicke G, Threton BM, Golden N, Datta PK, Roy CJ, Bohm RP, Maness NJ, Fischer T, Rappaport J, Vaccari M. 2020. Cellular events of acute, resolving, or progressive COVID-19 in SARS-CoV-2-infected nonhuman primates. *Nat Commun* 11:6078. <https://doi.org/10.1038/s41467-020-19967-4>.
  59. Ferrando C, Suarez-Sipmann F, Mellado-Artigas R, Hernández M, Gea A, Arruti E, Aldecoa C, Martínez-Pallí G, Martínez-González MA, Slutsky AS, Villar J; COVID-19 Spanish ICU Network. 2020. Clinical features, ventilatory management, and outcome of ARDS caused by COVID-19 are similar to other causes of ARDS. *Intensive Care Med* 46:2200–2211. <https://doi.org/10.1007/s00134-020-06192-2>.
  60. Fox SE, Akmatbekov A, Harbert JL, Li G, Brown JQ, Heide RSV. 2020. Pulmonary and cardiac pathology in African American patients with COVID-19: an autopsy series from New Orleans. *Lancet Respir Med* 8:681–686. [https://doi.org/10.1016/S2213-2600\(20\)30243-5](https://doi.org/10.1016/S2213-2600(20)30243-5).
  61. Gando S, Wada T. 2022. Pathomechanisms underlying hypoxemia in 2 COVID-19-associated acute respiratory distress syndrome phenotypes: Insights from thrombosis and hemostasis. *Shock* 57:1–6. <https://doi.org/10.1097/SHK.0000000000001825>.
  62. Gao CA, Bailey JI, Walter JM, Coleman JM, Malsin ES, Argento AC, Prickett MH, Wunderink RG, Smith SB. 2021. Bronchoscopy on intubated patients with COVID-19 is associated with low infectious risk to operators. *Ann Am Thorac Soc* 18:1243–1246. <https://doi.org/10.1513/AnnalsATS.202009-1225RL>.
  63. Garg S, Kim L, Whitaker M, O'Halloran A, Cummings C, Holstein R, Prill M, Chai SJ, Kirley PD, Alden NB, Kawasaki B, Yousey-Hindes K, Nicolai L, Anderson EJ, Openo KP, Weigel A, Monroe ML, Ryan P, Henderson J, Kim S, Como-Sabetti K, Lynfield R, Sosin D, Torres S, Muse A, Bennett NM, Billing L, Sutton M, West N, Schaffner W, Talbot HK, Aquino C, George A, Budd A, Brammer L, Langley G, Hall AJ, Fry A. 2020. Hospitalization rates and characteristics of patients hospitalized with laboratory-confirmed coronavirus disease 2019—COVID-NET, 14 states, March 1–30, 2020. *MMWR Morb Mortal Wkly Rep* 69:458–464. <https://doi.org/10.15585/mmwr.mm6915e3>.
  64. Gattinoni L, Chiumello D, Caironi P, Busana M, Romitti F, Brazzi L, Camporota L. 2020. COVID-19 pneumonia: Different respiratory treatments for different phenotypes? *Intensive Care Med* 46:1099–1102. <https://doi.org/10.1007/s00134-020-06033-2>.
  65. Gelardes I, Nguyen J, Gao J, Chen Q, Morales-Nebreda L, Wunderink R, Li L, Chmiel JS, Hrisinko M, Marszalek L, Momnani S, Patel P, Sumugod R, Chao Q, Jennings LJ, Zembower TR, Ji P, Chen YH. 2021. Comprehensive evaluation of bronchoalveolar lavage from patients with severe COVID-19 and correlation with clinical outcomes. *Hum Pathol* 113:92–103. <https://doi.org/10.1016/j.humpath.2021.04.010>.
  66. Giani M, Seminati D, Lucchini A, Foti G, Pagni F. 2020. Exuberant plasmocytosis in bronchoalveolar lavage specimen of the first patient requiring extracorporeal membrane oxygenation for SARS-CoV-2 in Europe. *J Thorac Oncol* 15:e65–e66. <https://doi.org/10.1016/j.jtho.2020.03.008>.
  67. Golden JW, Cline CR, Zeng X, Garrison AR, Carey BD, Mucker EM, White LE, Shamblin JD, Brocato RL, Liu J, Babka AM, Rauch HB, Smith JM, Hollidge BS, Fitzpatrick C, Badger CV, Hooper JW. 2020. Human angiotensin-converting enzyme 2 transgenic mice infected with SARS-CoV-2 develop severe and fatal respiratory disease. *JCI Insight* 5:e142032. <https://doi.org/10.1172/jci.insight.142032>.
  68. Gonçalves A, Maisonnasse P, Donati F, Albert M, Behillil S, Contreras V, Naninck T, Marlin R, Solas C, Pizzorno A, Lemaitre J, Kahlaoui N, Terrier O, Ho Tsong Fang R, Enouf V, Dereuddre-Bosquet N, Brisebarre A, Touret F, Chapon C, Hoen B, Lina B, Rosa Calatrava M, de Lamballerie X, Mentré F, Le Grand R, van der Werf S, Guedj J. 2021. SARS-CoV-2 viral dynamics in nonhuman primates. *PLOS Comput Biol* 17:e1008785. <https://doi.org/10.1371/journal.pcbi.1008785>.
  69. Grant RA, Morales-Nebreda L, Markov NS, Swaminathan S, Querrey M, Guzman ER, Abbott DA, Donnelly HK, Donayre A, Goldberg IA, Klug ZM, Borkowski N, Lu Z, Kihshen H, Politanaska Y, Sichizya L, Kang M, Shilatifard A, Qi C, Lomasney JW, Argento AC, Kruser JM, Malsin ES, Pickens CO, Smith SB, Walter JM, Pawlowski AE, Schneider D, Nannapaneni P, Abdala-Valencia H, Bharat A, Gottardi CJ, Budinger GRS, Misharin AV, Singer BD, Wunderink RG; NU SCRIPT Study Investigators. 2021. Circuits between infected macrophages and T cells in SARS-CoV-2 pneumonia. *Nature* 590:635–641. <https://doi.org/10.1038/s41586-020-03148-w>.
  70. Grasselli G, Tonetti T, Protti A, Langer T, Girardis M, Bellani G, Laffey J, Carrafiello G, Carsana L, Rizzuto C, Zanella A, Scaravilli V, Pizzilli G, Grieco DL, Di Meglio L, de Pascale G, Lanza E, Monteduro F, Zompatori M, Filippini C, Locatelli F, Cecconi M, Fumagalli R, Nava S, Vincent JL, Antonelli M, Slutsky AS, Pesenti A, Ranieri VM. 2020. Pathophysiology of COVID-19-associated acute respiratory distress syndrome: A multicenter prospective observational study. *Lancet Respir Med* 8:1201–1208. [https://doi.org/10.1016/S2213-2600\(20\)30370-2](https://doi.org/10.1016/S2213-2600(20)30370-2).
  71. Grosse C, Grosse A, Salzer HJF, Dünser MW, Motz R, Langer R. 2020. Analysis of cardiopulmonary findings in COVID-19 fatalities: High incidence of pulmonary artery thrombi and acute suppurative bronchopneumonia. *Cardiovasc Pathol* 49:107263. <https://doi.org/10.1016/j.carpath.2020.107263>.
  72. Gu H, Chen Q, Yang G, He L, Fan H, Deng Y-Q, Wang Y, Teng Y, Zhao Z, Cui Y, Li Y, Li XF, Li J, Zhang NN, Yang X, Chen S,



- Guo Y, Zhao G, Wang X, Luo DY, Wang H, Yang X, Li Y, Han G, He Y, Zhou X, Geng S, Sheng X, Jiang S, Sun S, Qin CF, Zhou Y. 2020. Adaptation of SARS-CoV-2 in BALB/c mice for testing vaccine efficacy. *Science* 369:1603–1607. <https://doi.org/10.1126/science.abc4730>.
73. Guan W-J, Ni Z-Y, Hu Y, Liang W-H, Ou C-Q, He J-X, Liu L, Shan H, Lei C-L, Hui DSC, Du B, Li LJ, Zeng G, Yuen KY, Chen RC, Tang CL, Wang T, Chen PY, Xiang J, Li SY, Wang JL, Liang ZJ, Peng YX, Wei L, Liu Y, Hu YH, Peng P, Wang JM, Liu JY, Chen Z, Li G, Zheng ZJ, Qiu SQ, Luo J, Ye CJ, Zhu SY, Zhong NS; China Medical Treatment Expert Group for Covid-19. 2020. Clinical characteristics of coronavirus disease 2019 in China. *N Engl J Med* 382:1708–1720. <https://doi.org/10.1056/NEJMoa2002032>.
  74. Habashi NM, Camporota L, Gatto LA, Nieman G. 2021. Functional pathophysiology of SARS-CoV-2-induced acute lung injury and clinical implications. *J Appl Physiol* 130:877–891. <https://doi.org/10.1152/jappphysiol.00742.2020>.
  75. Hariri LP, North CM, Shih AR, Israel RA, Maley JH, Villalba JA, Vinarsky V, Rubin J, Okin DA, Sclafani A, Alladina JW, Griffith JW, Gillette MA, Raz Y, Richards CJ, Wong AK, Ly A, Hung YP, Chivukula RR, Petri CR, Calhoun TF, Brenner LN, Hibbert KA, Medoff BD, Hardin CC, Stone JR, Mino-Kenudson M. 2021. Lung histopathology in coronavirus disease 2019 as compared with severe acute respiratory syndrome and H1N1 influenza. *Chest* 159:73–84. <https://doi.org/10.1016/j.chest.2020.09.259>.
  76. Hartman AL, Nambulli S, McMillen CM, White AG, Tilston-Lunel NL, Albe JR, Cottle E, Dunn MD, Frye LJ, Gilliland TH, Olsen EL, O'Malley KJ, Schwarz MM, Tomko JA, Walker RC, Xia M, Hartman MS, Klein E, Scanga CA, Flynn JL, Klimstra WB, McElroy AK, Reed DS, Duprex WP. 2020. SARS-CoV-2 infection of African green monkeys results in mild respiratory disease discernible by PET-CT imaging and shedding of infectious virus from both respiratory and gastrointestinal tracts. *PLoS Pathog* 16:e1008903. <https://doi.org/10.1371/journal.ppat.1008903>.
  77. Hoffmann M, Kleine-Weber H, Schroeder S, Krüger N, Herrler T, Erichsen S, Schiergens TS, Herrler G, Wu N-H, Nitsche A, Müller MA, Drosten C, Pöhlmann S. 2020. SARS-CoV-2 cell entry depends on ACE2 and TMPRSS2 and is blocked by a clinically proven protease inhibitor. *Cell* 181:271–280. <https://doi.org/10.1016/j.cell.2020.02.052>.
  78. Hou YJ, Okuda K, Edwards CE, Martinez DR, Asakura T, Dinnon KH 3<sup>rd</sup>, Kato T, Lee RE, Yount BL, Mascenik TM, Chen G, Olivier KN, Ghio A, Tse LV, Leist SR, Gralinski LE, Schäfer A, Dang H, Gilmore R, Nakano S, Sun L, Fulcher ML, Livraghi-Butrico A, Nicely NI, Cameron M, Cameron C, Kelvin DJ, de Silva A, Margolis DM, Markmann A, Bartelt L, Zumwalt R, Martinez FJ, Salvatore SP, Borczuk A, Tata PR, Sontake V, Kimple A, Jaspers I, O'Neal WK, Randell SH, Boucher RC, Baric RS. 2020. SARS-CoV-2 reverse genetics reveals a variable infection gradient in the respiratory tract. *Cell* 182:429–446.e14. <https://doi.org/10.1016/j.cell.2020.05.042>.
  79. Hu B, Guo H, Zhou P, Shi Z-L. 2021. Characteristics of SARS-CoV-2 and COVID-19. *Nat Rev Microbiol* 19:141–154. <https://doi.org/10.1038/s41579-020-00459-7>.
  80. Hu Z, Song C, Xu C, Jin G, Chen Y, Xu X, Ma H, Chen W, Lin Y, Zheng Y, Wang J, Hu Z, Yi Y, Shen H. 2020. Clinical characteristics of 24 asymptomatic infections with COVID-19 screened among close contacts in Nanjing, China. *Sci China Life Sci* 63:706–711. <https://doi.org/10.1007/s11427-020-1661-4>.
  81. Huang C, Wang Y, Li X, Ren L, Zhao J, Hu Y, Zhang L, Fan G, Xu J, Gu X, Cheng Z, Yu T, Xia J, Wei Y, Wu W, Xie X, Yin W, Li H, Liu M, Xiao Y, Gao H, Guo L, Xie J, Wang G, Jiang R, Gao Z, Jin Q, Wang J, Cao B. 2020. Clinical features of patients infected with 2019 novel coronavirus in Wuhan, China. *Lancet* 395:497–506. [https://doi.org/10.1016/S0140-6736\(20\)30183-5](https://doi.org/10.1016/S0140-6736(20)30183-5).
  82. Hughes S, Troise O, Donaldson H, Mughal N, Moore LSP. 2020. Bacterial and fungal coinfection among hospitalized patients with COVID-19: A retrospective cohort study in a UK secondary-care setting. *Clin Microbiol Infect* 26:1395–1399. <https://doi.org/10.1016/j.cmi.2020.06.025>.
  83. Imai M, Iwatsuki-Horimoto K, Hatta M, Loeber S, Halfmann PJ, Nakajima N, Watanabe T, Ujije M, Takahashi K, Ito M, Yamada S, Fan S, Chiba S, Kuroda M, Guan L, Takada K, Armbrust T, Balogh A, Furusawa Y, Okuda M, Ueki H, Yasuhara A, Sakai-Tagawa Y, Lopes TJS, Kiso M, Yamayoshi S, Kinoshita N, Ohmagari N, Hattori SI, Takeda M, Mitsuya H, Kramer F, Suzuki T, Kawaoka Y. 2020. Syrian hamsters as a small animal model for SARS-CoV-2 infection and countermeasure development. *Proc Natl Acad Sci USA* 117:16587–16595. <https://doi.org/10.1073/pnas.2009799117>.
  84. Ishigaki H, Nakayama M, Kitagawa Y, Nguyen CT, Hayashi K, Shiohara M, Gotoh B, Itoh Y. 2021. Neutralizing antibody-dependent and -independent immune responses against SARS-CoV-2 in cynomolgus macaques. *Virology* 554:97–105. <https://doi.org/10.1016/j.virol.2020.12.013>.
  85. Johnston SC, Ricks KM, Jay A, Raymond JL, Rossi F, Zeng X, Scruggs J, Dyer D, Frick O, Koehler JW, Kuehnert PA, Clements TL, Shoemaker CJ, Coyne SR, Delp KL, Moore J, Berrier K, Esham H, Shamblyn J, Sifford W, Fiallos J, Klosterman L, Stevens S, White L, Bowling P, Garcia T, Jensen C, Ghering J, Nyakiti D, Bellanca S, Kearney B, Giles W, Alli N, Paz F, Akers K, Danner D, Barth J, Johnson JA, Durant M, Kim R, Hooper JW, Smith JM, Kugelman JR, Beitzel BF, Gibson KM, Pitt MLM, Minogue TD, Nalca A. 2021. Development of a coronavirus disease 2019 nonhuman primate model using airborne exposure. *PLoS One* 16:e0246366. <https://doi.org/10.1371/journal.pone.0246366>.
  86. Jonigk D, Werlein C, Acker T, Aepfelbacher M, Amann KU, Baretton G, Barth P, Bohle RM, Büttner A, Büttner R, Dettmeyer R, Eichhorn P, Elezkurtaj S, Esposito I, Evert K, Evert M, Fend F, Gaßler N, Gattenlöhner S, Glatzel M, Göbel H, Gradhand E, Hansen T, Hartmann A, Heinemann A, Heppner FL, Hilsenbeck J, Horst D, Kamp JC, Mall G, Märkl B, Ondruschka B, Pablik J, Pfefferle S, Quaa A, Radbruch H, Röcken C, Rosenwald A, Roth W, Rudelius M, Schirmacher P, Slotta-Huspenina J, Smith K, Sommer L, Stock K, Ströbel P, Strobl S, Titze U, Weirich G, Weis J, Werner M, Wickenhauser C, Wiech T, Wild P, Welte T, von Stillfried S, Boor P. 2022. Organ manifestations of COVID-19: What have we learned so far (not only) from autopsies? *Virchows Arch* 481:139–159. <https://doi.org/10.1007/s00428-022-03319-2>.
  87. Junqueira C, Crespo Á, Ranjbar S, de Lacerda LB, Lewandrowski M, Ingber J, Parry B, Ravid S, Clark S, Schrimpf MR, Ho F, Beakes C, Margolin J, Russell N, Kays K, Boucau J, Das Adhikari U, Vora SM, Leger V, Gehrke L, Henderson LA, Janssen E, Kwon D, Sander C, Abraham J, Goldberg MB, Wu H, Mehta G, Bell S, Goldfeld AE, Filbin MR, Lieberman J. 2022. FcγR-mediated SARS-CoV-2 infection of monocytes activates inflammation. *Nature* 606:576–584. <https://doi.org/10.1038/s41586-022-04702-4>.
  88. Kao K-C, Hu H-C, Chang C-H, Hung C-Y, Chiu L-C, Li S-H, Lin S-W, Chang L-P, Wang C-W, Li L-F, Chen NH, Yang CT, Huang CC, Tsai YH. 2015. Diffuse alveolar damage associated mortality in selected acute respiratory distress syndrome patients with open lung biopsy. *Crit Care* 19:228. <https://doi.org/10.1186/s13054-015-0949-y>.
  89. Klein F, Soriano JC, Anfuso MB, Ruiz V, Perazzo M, Paladini H, Vigliano A, Ossés J, Lowenstein P, Vigliano C, Cánava J. 2021. Transbronchial biopsies' histopathological findings leading to successful late steroid therapy in Covid-19 acute respiratory failure. *Virchows Arch* 479:827–833. <https://doi.org/10.1007/s00428-020-02975-6>.
  90. Knight AC, Montgomery SA, Fletcher CA, Baxter VK. 2021. Mouse models for the study of SARS-CoV-2 infection. *Comp Med* 71:383–397. <https://doi.org/10.30802/AALAS-CM-21-000031>.
  91. Konopka KE, Nguyen T, Jentzen JM, Rayes O, Schmidt CJ, Wilson AM, Farver CF, Myers JL. 2020. Diffuse alveolar damage (DAD) resulting from coronavirus disease 2019 Infection is morphologically indistinguishable from other causes of DAD. *Histopathology* 77:570–578. <https://doi.org/10.1111/his.14180>.
  92. Koo B-S, Oh H, Kim G, Hwang E-H, Jung H, Lee Y, Kang P, Park J-H, Ryu C-M, Hong JJ. 2020. Transient lymphopenia and interstitial pneumonia with endotheliitis in SARS-CoV-2-infected macaques. *J Infect Dis* 222:1596–1600. <https://doi.org/10.1093/infdis/jiaa486>.
  93. Koppurapu VS, Puliaiev M, Doerschug KC, Schmidt GA. 2021. Ventilated patients with COVID-19 show airflow obstruction.



- tion. *J Intensive Care Med* 36:696–703. <https://doi.org/10.1177/08850666211000601>.
94. Lakshmanappa YS, Elizaldi SR, Roh JW, Schmidt BA, Carroll TD, Weaver KD, Smith JC, Verma A, Deere JD, Dutra J, Stone M, Franz S, Sammak RL, Olstad KJ, Rachel Reader J, Ma ZM, Nguyen NK, Watanabe J, Usachenko J, Immareddy R, Yee JL, Weiskopf D, Sette A, Hartigan-O'Connor D, McSorley SJ, Morrison JH, Tran NK, Simmons G, Busch MP, Kozlowski PA, Van Rompay KKA, Miller CJ, Iyer SS. 2021. SARS-CoV-2 induces robust germinal center CD4 T follicular helper cell responses in rhesus macaques. *Nat Commun* 12:541. <https://doi.org/10.1038/s41467-020-20642-x>.
95. Lamers MM, Haagmans BL. 2022. SARS-CoV-2 pathogenesis. *Nat Rev Microbiol* 20:270–284. <https://doi.org/10.1038/s41579-022-00713-0>.
96. Lamers MM, van der Vaart J, Knoop K, Riesebosch S, Breugem TI, Mykityn AZ, Beumer J, Schipper D, Bezstarosti K, Koopman CD, Groen N, Ravelli RBG, Duimel HQ, Demmers JAA, Verjans GMGM, Koopmans MPG, Muraro MJ, Peters PJ, Clevers H, Haagmans BL. 2021. An organoid-derived bronchioalveolar model for SARS-CoV-2 infection of human alveolar type II-like cells. *EMBO J* 40:e105912. <https://doi.org/10.15252/embj.2020105912>.
97. Lang M, Som A, Mendoza DP, Flores EJ, Reid N, Carey D, Li MD, Witkin A, Rodriguez-Lopez JM, Shepard J-AO, Little BP. 2020. Hypoxaemia related to COVID-19: vascular and perfusion abnormalities on dual-energy CT. *Lancet Infect Dis* 20:1365–1366. [https://doi.org/10.1016/S1473-3099\(20\)30367-4](https://doi.org/10.1016/S1473-3099(20)30367-4).
98. Lauer SA, Grantz KH, Bi Q, Jones FK, Zheng Q, Meredith HR, Azman AS, Reich NG, Lessler J. 2020. The incubation period of coronavirus disease 2019 (COVID-19) from publicly reported confirmed cases: Estimation and application. *Ann Intern Med* 172:577–582. <https://doi.org/10.7326/M20-0504>.
99. Lax SF, Skok K, Zechner P, Kessler HH, Kaufmann N, Koelblinger C, Vander K, Bargfrieder U, Trauner M. 2020. Pulmonary arterial thrombosis in COVID-19 with fatal outcome: Results from a prospective, single-center, clinicopathologic case series. *Ann Intern Med* 173:350–361. <https://doi.org/10.7326/M20-2566>.
100. Leist SR, Dinnon KH, Schäfer A, Tse LV, Okuda K, Hou YJ, West A, Edwards CE, Sanders W, Fritch EJ, et al. 2020. A mouse-adapted SARS-CoV-2 induces acute lung injury and mortality in standard laboratory mice. *Cell* 183:1070–1085.e12. <https://doi.org/10.1016/j.cell.2020.09.050>.
101. Levi M, Thachil J, Iba T, Levy JH. 2020. Coagulation abnormalities and thrombosis in patients with COVID-19. *Lancet Haematol* 7:e438–e440. [https://doi.org/10.1016/S2352-3026\(20\)30145-9](https://doi.org/10.1016/S2352-3026(20)30145-9).
102. Li Y, Wu J, Wang S, Li X, Zhou J, Huang B, Luo D, Cao Q, Chen Y, Chen S, Ma L, Peng L, Pan H, Travis WD, Nie X. 2021. Progression to fibrosing diffuse alveolar damage in a series of 30 minimally invasive autopsies with COVID-19 pneumonia in Wuhan, China. *Histopathology* 78:542–555. <https://doi.org/10.1111/his.14249>.
103. Liao M, Liu Y, Yuan J, Wen Y, Xu G, Zhao J, Cheng L, Li J, Wang X, Wang F, Liu L, Amit I, Zhang S, Zhang Z. 2020. Single-cell landscape of bronchioalveolar immune cells in patients with COVID-19. *Nat Med* 26:842–844. <https://doi.org/10.1038/s41591-020-0901-9>.
104. Liu F, Han K, Blair R, Kenst K, Qin Z, Upcin B, Wörsdörfer P, Midkiff CC, Mudd J, Belyaeva E, Milligan NS, Rorison TD, Wagner N, Bodem J, Dölken L, Aktas BH, Vander Heide RS, Yin XM, Kolls JK, Roy CJ, Rappaport J, Ergün S, Qin X. 2021. SARS-CoV-2 infects endothelial cells in vivo and in vitro. *Front Cell Infect Microbiol* 11:701278. <https://doi.org/10.3389/fcimb.2021.701278>.
105. Liu Q, Shi Y, Cai J, Duan Y, Wang R, Zhang H, Ruan Q, Li J, Zhao L, Ping Y, Chen R, Ren L, Fei X, Zhang H, Tang R, Wang X, Luo T, Liu X, Huang X, Liu Z, Ao Q, Ren Y, Xiong J, He Z, Wu H, Fu W, Zhao P, Chen X, Qu G, Wang Y, Wang X, Liu J, Xiang D, Xu S, Zhou X, Li Q, Ma J, Li H, Zhang J, Huang S, Yao X, Zhou Y, Wang C, Zhang D, Wang G, Liu L, Bian XW. 2020. Pathological changes in the lungs and lymphatic organs of 12 COVID-19 autopsy cases. *Natl Sci Rev* 7:1868–1878. <https://doi.org/10.1093/nsr/nwaa247>.
106. Lu S, Zhao Y, Yu W, Yang Y, Gao J, Wang J, Kuang D, Yang M, Yang J, Ma C, Xu J, Qian X, Li H, Zhao S, Li J, Wang H, Long H, Zhou J, Luo F, Ding K, Wu D, Zhang Y, Dong Y, Liu Y, Zheng Y, Lin X, Jiao L, Zheng H, Dai Q, Sun Q, Hu Y, Ke C, Liu H, Peng X. 2020. Comparison of nonhuman primates identified the suitable model for COVID-19. *Signal Transduct Target Ther* 5:157. <https://doi.org/10.1038/s41392-020-00269-6>.
107. de Maat S, de Mast Q, Danser AHJ, van de Veerdonk FL, Maas C. 2020. Impaired breakdown of bradykinin and its metabolites as a possible cause for pulmonary edema in COVID-19 infection. *Semin Thromb Hemost* 46:835–837. <https://doi.org/10.1055/s-0040-1712960>.
108. Maisonnasse P, Guedj J, Contreras V, Behillil S, Solas C, Marlin R, Naninck T, Pizzorno A, Lemaître J, Gonçalves A, Kahlaoui N, Terrier O, Fang RHT, Enouf V, Dereuddre-Bosquet N, Brisebarre A, Touret F, Chapon C, Hoen B, Lina B, Calatrava MR, van der Werf S, de Lamballerie X, Le Grand R. 2020. Hydroxychloroquine use against SARS-CoV-2 infection in non-human primates. *Nature* 585:584–587. <https://doi.org/10.1038/s41586-020-2558-4>.
109. Martines RB, Ritter JM, Matkovic E, Gary J, Bollweg BC, Bullock H, Goldsmith CS, Silva-Flannery L, Seixas JN, Reagan-Steiner S, Uyeki T, Denison A, Bhatnagar J, Shieh WJ, Zaki SR; COVID-19 Pathology Working Group. 2020. Pathology and pathogenesis of SARS-CoV-2 associated with fatal coronavirus disease, United States. *Emerg Infect Dis* 26:2005–2015. <https://doi.org/10.3201/eid2609.202095>.
110. Matute-Bello G, Downey G, Moore BB, Groshong SD, Matthay MA, Slutsky AS, Kuebler WM, Group ALI. 2011. An official American Thoracic Society workshop report: Features and measurements of experimental acute lung injury in animals. *Am J Respir Cell Mol Biol* 44:725–738. <https://doi.org/10.1165/rcmb.2009-0210ST>.
111. Maucourant C, Filipovic I, Ponzetta A, Aleman S, Cornillet M, Hertwig L, Strunz B, Lentini A, Reinius B, Brownlie D, Cuapio A, Ask EH, Hull RM, Haroun-Izquierdo A, Schaffer M, Klingström J, Folkesson E, Buggert M, Sandberg JK, Eriksson LI, Rooyackers O, Ljunggren HG, Malmberg KJ, Michaëlsen S, Marquardt N, Hammer Q, Strålin K, Björkström NK; Karolinska COVID-19 Study Group. 2020. Natural killer cell immunotypes related to COVID-19 disease severity. *Sci Immunol* 5:eabd6832. <https://doi.org/10.1126/sciimmunol.abd6832>.
112. McCray PB, Pewe L, Wohlford-Lenane C, Hickey M, Manzel L, Shi L, Netland J, Jia HP, Halabi C, Sigmund CD, Meyerholz DK, Kirby P, Look DC, Perlman S. 2007. Lethal infection of K18-hACE2 mice infected with severe acute respiratory syndrome coronavirus. *J Virol* 81:813–821. <https://doi.org/10.1128/JVI.02012-06>.
113. Melms JC, Biermann J, Huang H, Wang Y, Nair A, Tagore S, Katsyv I, Rendeiro AF, Amin AD, Schapiro D, Frangieh CJ, Luoma AM, Filliol A, Fang Y, Ravichandran H, Clausi MG, Alba GA, Rogava M, Chen SW, Ho P, Montoro DT, Kornberg AE, Han AS, Bakhom MF, Anandasabapathy N, Suárez-Fariñas M, Bakhom SF, Bram Y, Borczuk A, Guo XV, Lefkowitz JH, Marboe C, Lagana SM, Del Portillo A, Tsai EJ, Zorn E, Markowitz GS, Schwabe RF, Schwartz RE, Elemento O, Saqi A, Hibshoosh H, Que J, Izar B. 2021. A molecular single-cell lung atlas of lethal COVID-19. *Nature* 595:114–119. <https://doi.org/10.1038/s41586-021-03569-1>.
114. Menachery VD, Gralinski LE, Baric RS, Ferris MT. 2015. New Metrics for Evaluating Viral Respiratory Pathogenesis. *PLoS One* 10:e0131451. <https://doi.org/10.1371/journal.pone.0131451>.
115. Menter T, Haslbauer JD, Nienhold R, Savic S, Hopfer H, Deigendesch N, Frank S, Turek D, Willi N, Pargger H, Bassetti S, Leuppi JD, Cathomas G, Tolnay M, Mertz KD, Tzankov A. 2020. Postmortem examination of COVID-19 patients reveals diffuse alveolar damage with severe capillary congestion and variegated findings in lungs and other organs suggesting vascular dysfunction. *Histopathology* 77:198–209. <https://doi.org/10.1111/his.14134>.
116. Michele SD, Sun Y, Yilmaz MM, Katsyv I, Salvatore M, Dzierba AL, Marboe CC, Brodie D, Patel NM, Garcia CK, Saqi A. 2020. Forty postmortem examinations in COVID-19 patients. *Am J Clin Pathol* 154:748–760. <https://doi.org/10.1093/ajcp/aqaa156>.
117. Middleton EA, He X-Y, Denorme F, Campbell RA, Ng D, Salvatore SP, Mostycka M, Baxter-Stoltzfus A, Borczuk AC, Loda M, Cody MJ, Manne BK, Portier I, Harris ES, Petrey AC, Beswick EJ, Caulin AF, Iovino A, Abegglen LM, Weyrich AS, Rondina MT, Egeblad M, Schiffman JD, Yost CC. 2020. Neutrophil extracel-

- lular traps contribute to immunothrombosis in COVID-19 acute respiratory distress syndrome. *Blood* **136**:1169–1179. <https://doi.org/10.1182/blood.2020007008>.
118. Milross L, Majo J, Cooper N, Kaye PM, Bayraktar O, Filby A, Fisher AJ. 2022. Postmortem lung tissue: the fossil record of the pathophysiology and immunopathology of severe COVID-19. *Lancet Respir Med* **10**:95–106. [https://doi.org/10.1016/S2213-2600\(21\)00408-2](https://doi.org/10.1016/S2213-2600(21)00408-2).
  119. Mohanty SK, Satapathy A, Naidu MM, Mukhopadhyay S, Sharma S, Barton LM, Stroberg E, Duval EJ, Pradhan D, Tzankov A, Parwani AV. 2020. Severe acute respiratory syndrome coronavirus-2 (SARS-CoV-2) and coronavirus disease 19 (COVID-19)—anatomic pathology perspective on current knowledge. *Diagn Pathol* **15**:103. <https://doi.org/10.1186/s13000-020-01017-8>.
  120. Muñoz-Fontela C, Dowling WE, Funnell SGP, Gsell P-S, Riveros-Balta AX, Albrecht RA, Andersen H, Baric RS, Carroll MW, Cavaleri M, Qin C, Crozier I, Dallmeier K, de Waal L, de Wit E, Delang L, Dohm E, Duprex WP, Falzarano D, Finch CL, Frieman MB, Graham BS, Gralinski LE, Guilfoyle K, Haagmans BL, Hamilton GA, Hartman AL, Herfst S, Kaptein SJF, Klimstra WB, Knezevic I, Krause PR, Kuhn JH, Le Grand R, Lewis MG, Liu WC, Maisonnasse P, McElroy AK, Munster V, Oreshkova N, Rasmussen AL, Rocha-Pereira J, Rockx B, Rodríguez E, Rogers TF, Salguero FJ, Schotsaert M, Stittelaar KJ, Thibaut HJ, Tseng CT, Vergara-Alert J, Beer M, Brasel T, Chan JFW, García-Sastre A, Neyts J, Perlman S, Reed DS, Richt JA, Roy CJ, Segalés J, Vasan SS, Henao-Restrepo AM, Barouch DH. 2020. Animal models for COVID-19. *Nature* **586**:509–515. <https://doi.org/10.1038/s41586-020-2787-6>.
  121. Munster VJ, Feldmann F, Williamson BN, van Doremalen N, Pérez-Pérez L, Schulz J, Meade-White K, Okumura A, Callison J, Brumbaugh B, Avanzato VA, Rosenke R, Hanley PW, Saturday G, Scott D, Fischer ER, de Wit E. 2020. Respiratory disease in rhesus macaques inoculated with SARS-CoV-2. *Nature* **585**:268–272. <https://doi.org/10.1038/s41586-020-2324-7>.
  122. Muruato A, Vu MN, Johnson BA, Davis-Gardner ME, Vanderheiden A, Lokugamage K, Schindewolf C, Crocquet-Valdes PA, Langsjoen RM, Plante JA, Plante KS, Weaver SC, Debbink K, Routh AL, Walker D, Suthar MS, Shi PY, Xie X, Menachery VD. 2021. Mouse-adapted SARS-CoV-2 protects animals from lethal SARS-CoV challenge. *PLoS Biol* **19**:e3001284. <https://doi.org/10.1371/journal.pbio.3001284>.
  123. Nakayama T, Lee IT, Jiang S, Matter MS, Yan CH, Overdevest JB, Wu C-T, Goltsev Y, Shih L-C, Liao C-K, Zhu B, Bai Y, Lidsky P, Xiao Y, Zarabanda D, Yang A, Easwaran M, Schürch CM, Chu P, Chen H, Stalder AK, McIlwain DR, Borchard NA, Gall PA, Dholakia SS, Le W, Xu L, Tai CJ, Yeh TH, Erickson-Direnzo E, Duran JM, Mertz KD, Hwang PH, Haslbauer JD, Jackson PK, Menter T, Andino R, Canoll PD, DeConde AS, Patel ZM, Tzankov A, Nolan GP, Nayak JV. 2021. Determinants of SARS-CoV-2 entry and replication in airway mucosal tissue and susceptibility in smokers. *Cell Rep Med* **2**:100421. <https://doi.org/10.1016/j.xcrm.2021.100421>.
  124. Nasa P, Azoulay E, Khanna AK, Jain R, Gupta S, Javeri Y, Juneja D, Rangappa P, Sundararajan K, Alhazzani W, Antonelli M, Arabi YM, Bakker J, Brochard LJ, Deane AM, Du B, Einav S, Esteban A, Gajic O, Galvagno SM Jr, Guérin C, Jaber S, Khilnani GC, Koh Y, Lascarrou JB, Machado FR, Malbrain MLNG, Mancebo J, McCurdy MT, McGrath BA, Mehta S, Mekontso-Dessap A, Mer M, Nurok M, Park PK, Pelosi P, Peter JV, Phua J, Pilcher DV, Piquilloud L, Schellongowski P, Schultz MJ, Shankar-Hari M, Singh S, Sorbello M, Tiruvoipati R, Udy AA, Welte T, Myatra SN. 2021. Expert consensus statements for the management of COVID-19-related acute respiratory failure using a Delphi method. *Crit Care* **25**:106. <https://doi.org/10.1186/s13054-021-03491-y>.
  125. Nicolai L, Leunig A, Brambs S, Kaiser R, Joppich M, Hoffknecht M, Gold C, Engel A, Polewka V, Muenchhoff M, Hellmuth JC, Ruhle A, Ledderose S, Weinberger T, Schulz H, Scherer C, Rudelius M, Zoller M, Keppler OT, Zwißler B, von Bergwelt-Baildon M, Kääh S, Zimmer R, Bülow RD, von Stillfried S, Boor P, Massberg S, Pekayvaz K, Stark K. 2021. Vascular neutrophilic inflammation and immunothrombosis distinguish severe COVID-19 from influenza pneumonia. *J Thromb Haemost* **19**:574–581. <https://doi.org/10.1111/jth.15179>.
  126. Nicolai L, Leunig A, Brambs S, Kaiser R, Weinberger T, Weigand M, Muenchhoff M, Hellmuth JC, Ledderose S, Schulz H, Scherer C, Rudelius M, Zoller M, Höchter D, Keppler O, Teupser D, Zwißler B, von Bergwelt-Baildon M, Kääh S, Massberg S, Pekayvaz K, Stark K. 2020. Immunothrombotic dysregulation in COVID-19 pneumonia is associated with respiratory failure and coagulopathy. *Circulation* **142**:1176–1189. <https://doi.org/10.1161/CIRCULATIONAHA.120.048488>.
  127. Osterrieder N, Bertzbach LD, Dietert K, Abdelgawad A, Vladimirova D, Kunec D, Hoffmann D, Beer M, Gruber AD, Trimper J. 2020. Age-dependent progression of SARS-CoV-2 infection in Syrian hamsters. *Viruses* **12**:779. <https://doi.org/10.3390/v12070779>.
  128. Osuchowski MF, Winkler MS, Skirecki T, Cajander S, Shankar-Hari M, Lachmann G, Monnet G, Venet F, Bauer M, Brunkhorst FM, Weis S, Garcia-Salido A, Kox M, Cavaillon JM, Uhle F, Weigand MA, Flohé SB, Wiersinga WJ, Almansa R, de la Fuente A, Martin-Loeches I, Meisel C, Spinetti T, Schefold JC, Cilloniz C, Torres A, Giamarellos-Bourboulis EJ, Ferrer R, Girardis M, Cossarizza A, Netea MG, van der Poll T, Bermejo-Martín JF, Rubio I. 2021. The COVID-19 puzzle: Deciphering pathophysiology and phenotypes of a new disease entity. *Lancet Respir Med* **9**:622–642. [https://doi.org/10.1016/S2213-2600\(21\)00218-6](https://doi.org/10.1016/S2213-2600(21)00218-6).
  129. Pagnesi M, Baldetti L, Beneduce A, Calvo F, Gramegna M, Pazzanese V, Ingallina G, Napolano A, Finazzi R, Ruggeri A, Ajello S, Melisurgo G, Camici PG, Scarpellini P, Tresoldi M, Landoni G, Ciceri F, Scandroglio AM, Agricola E, Cappelletti AM. 2020. Pulmonary hypertension and right ventricular involvement in hospitalized patients with COVID-19. *Heart* **106**:1324–1331. <https://doi.org/10.1136/heartjnl-2020-317355>.
  130. Panwar R, Madotto F, Laffey JG, van Haren FMP. 2020. Compliance phenotypes in early acute respiratory distress syndrome before the COVID-19 pandemic. *Am J Respir Crit Care Med* **202**:1244–1252. <https://doi.org/10.1164/rccm.202005-2046OC>.
  131. Park WY, Goodman RB, Steinberg KP, Ruzinkski JT, Il FR, Park DR, Pugin J, Skerrett SJ, Hudson LD, Martin TR. 2001. Cytokine balance in the lungs of patients with acute respiratory distress syndrome. *Am J Respir Crit Care Med* **164**:1896–1903. <https://doi.org/10.1164/ajrccm.164.10.2104013>.
  132. Patel BV, Arachchilage DJ, Ridge CA, Bianchi P, Doyle JF, Garfield B, Ledot S, Morgan C, Passariello M, Price S, Singh S, Thakuria L, Trenfield S, Trimlett R, Weaver C, Wort SJ, Xu T, Padley SPG, Devaraj A, Desai SR. 2020. Pulmonary angiopathy in severe COVID-19: Physiologic, imaging, and hematologic observations. *Am J Respir Crit Care Med* **202**:690–699. <https://doi.org/10.1164/rccm.202004-1412OC>.
  133. Pernazza A, Mancini M, Rullo E, Bassi M, Giacomo TD, Rocca CD, d'Amati G. 2020. Early histologic findings of pulmonary SARS-CoV-2 infection detected in a surgical specimen. *Virchows Arch* **477**:743–748. <https://doi.org/10.1007/s00428-020-02829-1>.
  134. Polak SB, Gool ICV, Cohen D, von der Thüsen JH, van Paassen J. 2020. A systematic review of pathological findings in COVID-19: a pathophysiological timeline and possible mechanisms of disease progression. *Mod Pathol* **33**:2128–2138. <https://doi.org/10.1038/s41379-020-0603-3>.
  135. Radermecker C, Detrembleur N, Guiot J, Cavalier E, Henket M, d'Emal C, Vanwinge C, Cataldo D, Oury C, Delvenne P, Marichal T. 2020. Neutrophil extracellular traps infiltrate the lung airway, interstitial, and vascular compartments in severe COVID-19. *J Exp Med* **217**:e20201012. <https://doi.org/10.1084/jem.20201012>.
  136. Rathnasinghe R, Strohmeier S, Amanat F, Gillespie VL, Krammer F, García-Sastre A, Coughlan L, Schotsaert M, Uccellini MB. 2020. Comparison of transgenic and adenovirus hACE2 mouse models for SARS-CoV-2 infection. *Emerg Microbes Infect* **9**:2433–2445. <https://doi.org/10.1080/22221751.2020.1838955>.
  137. Richardson S, Hirsch JS, Narasimhan M, Crawford JM, McGinn T, Davidson KW, The Northwell COVID-19 Research Consortium, Barnaby DP, Becker LB, Chelico JD, Cohen SL, Cookingham



- J, Coppa K, Diefenbach MA, Dominello AJ, Duer-Hefe J, Falzon L, Gitlin J, Hajizadeh N, Harvin TG, Hirschwerk DA, Kim EJ, Kozel ZM, Marrast LM, Mogavero JN, Osorio GA, Qiu M, Zanos TP. 2020. Presenting characteristics, comorbidities, and outcomes among 5700 patients hospitalized with COVID-19 in the New York City Area. *JAMA* 323:2052–2059. <https://doi.org/10.1001/jama.2020.6775>.
138. Rockx B, Kuiken T, Herfst S, Bestebroer T, Lamers MM, Munnink BBO, de Meulder D, van Amerongen G, van den Brand J, Okba NMA, Schipper D, van Run P, Leijten L, Sikkema R, Verschoor E, Verstrepen B, Bogers W, Langermans J, Drosten C, Fentener van Vlissingen M, Fouchier R, de Swart R, Koopmans M, Haagmans BL. 2020. Comparative pathogenesis of COVID-19, MERS, and SARS in a nonhuman primate model. *Science* 368:1012–1015. <https://doi.org/10.1126/science.abb7314>.
139. Rosa BA, Ahmed M, Singh DK, Choreño-Parra JA, Cole J, Jiménez-Álvarez LA, Rodríguez-Reyna TS, Singh B, Gonzalez O, Carrion R Jr, Schlesinger LS, Martin J, Zúñiga J, Mitreva M, Kaushal D, Khader SA. 2021. IFN signaling and neutrophil degranulation transcriptional signatures are induced during SARS-CoV-2 infection. *Commun Biol* 4:290. <https://doi.org/10.1038/s42003-021-01829-4>.
140. Rosenke K, Meade-White K, Letko M, Clancy C, Hansen F, Liu Y, Okumura A, Tang-Huau T-L, Li R, Saturday G, Feldmann F, Scott D, Wang Z, Munster V, Jarvis MA, Feldmann H. 2020. Defining the Syrian hamster as a highly susceptible preclinical model for SARS-CoV-2 infection. *Emerg Microbes Infect* 9:2673–2684. <https://doi.org/10.1080/22221751.2020.1858177>.
141. Roussel M, Ferrant J, Reizine F, Gallou SL, Dulong J, Carl S, Lesouhaitier M, Gregoire M, Bescher N, Verdy C, Latour M, Bézier I, Cornic M, Vinit A, Monvoisin C, Sawitzki B, Leonard S, Paul S, Feuillard J, Jeannot R, Daix T, Tiwari VK, Tadié JM, Cogné M, Tarte K. 2021. Comparative immune profiling of acute respiratory distress syndrome patients with or without SARS-CoV-2 infection. *Cell Rep Med* 2:100291. <https://doi.org/10.1016/j.xcrim.2021.100291>.
142. Rovas A, Osiaevi I, Buscher K, Sackarnd J, Tepas P-R, Fobker M, Kühn J, Braune S, Göbel U, Thölking G, Gröschel A, Pavenstädt H, Vink H, Kümpers P. 2021. Microvascular dysfunction in COVID-19: The MYSTIC study. *Angiogenesis* 24:145–157. <https://doi.org/10.1007/s10456-020-09753-7>.
143. Ruiz-Bedoya CA, Mota F, Ordonez AA, Foss CA, Singh AK, Praharaj M, Mahmud FJ, Ghayoor A, Flavahan K, Jesus PD, Bahr M, Dhakal S, Zhou R, Solis CV, Mulka KR, Bishai WR, Pekosz A, Mankowski JL, Villano J, Klein SL, Jain SK. 2022. <sup>124</sup>I-Iodo-DPA-713 positron emission tomography in a hamster model of SARS-CoV-2 infection. *Mol Imaging Biol* 24:135–143. <https://doi.org/10.1007/s11307-021-01638-5>.
144. Salguero FJ, White AD, Slack GS, Fotheringham SA, Bewley KR, Gooch KE, Longet S, Humphries HE, Watson RJ, Hunter L, Ryan KA, Hall Y, Sibley L, Sarfas C, Allen L, Aram M, Brunt E, Brown P, Buttigieg KR, Cavell BE, Cobb R, Coombes NS, Darby A, Daykin-Pont O, Elmoro MJ, Garcia-Dorival I, Gkolfinos K, Godwin KJ, Gouriet J, Halkerston R, Harris DJ, Hender T, Ho CMK, Kennard CL, Knott D, Leung S, Lucas V, Mabbutt A, Morrison AL, Nelson C, Ngabo D, Paterson J, Penn EJ, Pullan S, Taylor I, Tipton T, Thomas S, Tree JA, Turner C, Vamos E, Wand N, Wiblin NR, Charlton S, Dong X, Hallis B, Pearson G, Rayner EL, Nicholson AG, Funnell SG, Hiscox JA, Dennis MJ, Gleeson FV, Sharpe S, Carroll MW. 2021. Comparison of rhesus and cynomolgus macaques as an infection model for COVID-19. *Nat Commun* 12:1260. <https://doi.org/10.1038/s41467-021-21389-9>.
145. Santamarina MG, Riscal DB, Beddings I, Contreras R, Baque M, Volpacchio M, Lomakin FM. 2020. COVID-19: What iodine maps from perfusion CT can reveal—A prospective cohort study. *Crit Care* 24:619. <https://doi.org/10.1186/s13054-020-03333-3>.
146. Sauter JL, Baine MK, Butnor KJ, Buonocore DJ, Chang JC, Jungbluth AA, Szabolcs MJ, Morjaria S, Mount SL, Rekhtman N, Selbs E, Sheng ZM, Xiao Y, Kleiner DE, Pittaluga S, Taubenberger JK, Rapkiewicz AV, Travis WD. 2020. Insights into pathogenesis of fatal COVID-19 pneumonia from histopathology with immunohistochemical and viral RNA studies. *Histopathology* 77:915–925. <https://doi.org/10.1111/his.14201>.
147. Scardapane A, Villani L, Bavaro DF, Passerini F, Ianora AAS, Lucarelli NM, Angarano G, Portincasa P, Palmieri VO, Saracino A. 2021. Pulmonary Artery filling defects in COVID-19 patients revealed using CT pulmonary angiography: A predictable complication? *BioMed Res Int* 2021:8851736. <https://doi.org/10.1155/2021/8851736>.
148. Schmidt ME, Knudson CJ, Hartwig SM, Pewe LL, Meyerholz DK, Langlois RA, Harty JT, Varga SM. 2018. Memory CD8 T cells mediate severe immunopathology following respiratory syncytial virus infection. *PLoS Pathog* 14:e1006810. <https://doi.org/10.1371/journal.ppat.1006810>.
149. Schwensen HF, Borreschmidt LK, Storgaard M, Redsted S, Christensen S, Madsen LB. 2020. Fatal pulmonary fibrosis: A post-COVID-19 autopsy case. *J Clin Pathol* 74:400–402. <https://doi.org/10.1136/jclinpath-2020-206879>.
150. Sekulic M, Harper H, Nezami BG, Shen DL, Sekulic SP, Koeth AT, Harding CV, Gilmore H, Sadri N. 2020. Molecular detection of SARS-CoV-2 infection in FFPE samples and histopathologic findings in fatal SARS-CoV-2 cases. *Am J Clin Pathol* 154:190–200. <https://doi.org/10.1093/ajcp/aqaa091>.
151. Shan C, Yao Y-F, Yang X-L, Zhou Y-W, Gao G, Peng Y, Yang L, Hu X, Xiong J, Jiang R-D, Zhang HJ, Gao XX, Peng C, Min J, Chen Y, Si HR, Wu J, Zhou P, Wang YY, Wei HP, Pang W, Hu ZF, Lv LB, Zheng YT, Shi ZL, Yuan ZM. 2020. Infection with novel coronavirus (SARS-CoV-2) causes pneumonia in Rhesus macaques. *Cell Res* 30:670–677. <https://doi.org/10.1038/s41422-020-0364-z>.
152. Shang J, Wan Y, Luo C, Ye G, Geng Q, Auerbach A, Li F. 2020. Cell entry mechanisms of SARS-CoV-2. *Proc Natl Acad Sci USA* 117:11727–11734. <https://doi.org/10.1073/pnas.2003138117>.
153. Shi H, Han X, Jiang N, Cao Y, Alwalid O, Gu J, Fan Y, Zheng C. 2020. Radiological findings from 81 patients with COVID-19 pneumonia in Wuhan, China: a descriptive study. *Lancet Infect Dis* 20:425–434. [https://doi.org/10.1016/S1473-3099\(20\)30086-4](https://doi.org/10.1016/S1473-3099(20)30086-4).
154. Sia SF, Yan L-M, Chin AW, Fung K, Choy K-T, Wong AY, Kaewpreedee P, Perera RA, Poon LL, Nicholls JM, Peiris M, Yen HL. 2020. Pathogenesis and transmission of SARS-CoV-2 in golden hamsters. *Nature* 583:834–838. <https://doi.org/10.1038/s41586-020-2342-5>.
155. Singh DK, Singh B, Ganatra SR, Gazi M, Cole J, Thippeshappa R, Alfson KJ, Clemmons E, Gonzalez O, Escobedo R, Gough M, Alvarez C, Blakley A, Ferdin J, Bartley C, Staples H, Parodi L, Callery J, Mannino A, Klaffke B, Escareno P, Platt RN 2<sup>nd</sup>, Hodara V, Scordo J, Gautam S, Vilanova AG, Olmo-Fontanez A, Schami A, Oyejide A, Ajithdoss DK, Copin R, Baum A, Kyratsous C, Alvarez X, Ahmed M, Rosa B, Goodroe A, Dutton J, Hall-Urson S, Frost PA, Voges AK, Ross CN, Sayers K, Chen C, Hallam C, Khader SA, Mitreva M, Anderson TJC, Martinez-Sobrido L, Patterson JL, Turner J, Torrelles JB, Dick EJ Jr, Brasky K, Schlesinger LS, Giavedoni LD, Carrion R Jr, Kaushal D. 2021. Responses to acute infection with SARS-CoV-2 in the lungs of rhesus macaques, baboons and marmosets. *Nat Microbiol* 6:73–86. <https://doi.org/10.1038/s41564-020-00841-4>.
156. Song T-Z, Zheng H-Y, Han J-B, Jin L, Yang X, Liu F-L, Luo R-H, Tian R-R, Cai H-R, Feng X-L, Liu C, Li MH, Zheng YT. 2020. Delayed severe cytokine storm and immune cell infiltration in SARS-CoV-2-infected aged Chinese rhesus macaques. *Zool Res* 41:503–516. <https://doi.org/10.24272/j.issn.2095-8137.2020.202>.
157. Speranza E, Williamson BN, Feldmann F, Sturdevant GL, Pérez-Pérez LJ, Meade-White K, Smith BJ, Lovaglio J, Martens C, Munster VJ, Okumura A, Shaia C, Feldmann H, Best SM, de Wit E. 2021. Single-cell RNA sequencing reveals SARS-CoV-2 infection dynamics in lungs of African green monkeys. *Sci Transl Med* 13:eabe8146. <https://doi.org/10.1126/scitranslmed.abe8146>.
158. Stammes MA, Lee JH, Meijer L, Naninck T, Doyle-Meyers LA, White AG, Borish HJ, Hartman AL, Alvarez X, Ganatra S, Kaushal D, Bohm RP, le Grand R, Scanga CA, Langermans JAM, Bontrop RE, Finch CL, Flynn JL, Calcagno C, Crozier I, Kuhn JH. 2022. Medical imaging of pulmonary disease in SARS-CoV-



- 2-exposed non-human primates. *Trends Mol Med* **28**:123–142. <https://doi.org/10.1016/j.molmed.2021.12.001>.
159. Sun S, Gu H, Cao L, Chen Q, Ye Q, Yang G, Li R-T, Fan H, Deng Y-Q, Song X, Qi Y, Li M, Lan J, Feng R, Guo Y, Zhu N, Qin S, Wang L, Zhang YF, Zhou C, Zhao L, Chen Y, Shen M, Cui Y, Yang X, Wang X, Tan W, Wang H, Wang X, Qin CF. 2021. Characterization and structural basis of a lethal mouse-adapted SARS-CoV-2. *Nat Commun* **12**:5654. <https://doi.org/10.1038/s41467-021-25903-x>.
  160. Swenson KE, Swenson ER. 2021. Pathophysiology of acute respiratory distress syndrome and COVID-19 lung injury. *Crit Care Clin* **37**:749–776. <https://doi.org/10.1016/j.ccc.2021.05.003>.
  161. Tang N, Li D, Wang X, Sun Z. 2020. Abnormal coagulation parameters are associated with poor prognosis in patients with novel coronavirus pneumonia. *J Thromb Haemost* **18**:844–847. <https://doi.org/10.1111/jth.14768>.
  162. Tian S, Hu W, Niu L, Liu H, Xu H, Xiao S-Y. 2020. Pulmonary pathology of early-phase 2019 novel coronavirus (COVID-19) pneumonia in 2 patients with lung cancer. *J Thorac Oncol* **15**:700–704. <https://doi.org/10.1016/j.jtho.2020.02.010>.
  163. Tian S, Xiong Y, Liu H, Niu L, Guo J, Liao M, Xiao S-Y. 2020. Pathological study of the 2019 novel coronavirus disease (COVID-19) through postmortem core biopsies. *Mod Pathol* **33**:1007–1014. <https://doi.org/10.1038/s41379-020-0536-x>.
  164. Torres-Castro R, Vasconcello-Castillo L, Alsina-Restoy X, Solis-Navarro L, Burgos F, Puppo H, Vilaró J. 2021. Respiratory function in patients postinfection by COVID-19: A systematic review and meta-analysis. *Pulmonology* **27**:328–337. <https://doi.org/10.1016/j.pulmoe.2020.10.013>.
  165. Trichel AM. 2021. Overview of nonhuman primate models of SARS-CoV-2 infection. *Comp Med* **71**:411–432. <https://doi.org/10.30802/AALAS-CM-20-000119>.
  166. Urano E, Okamura T, Ono C, Ueno S, Nagata S, Kamada H, Higuchi M, Furukawa M, Kamitani W, Matsuura Y, Kawaoka Y, Yasutomi Y. 2021. COVID-19 cynomolgus macaque model reflecting human COVID-19 pathological conditions. *Proc Natl Acad Sci USA* **118**:e2104847118. <https://doi.org/10.1073/pnas.2104847118>.
  167. Valle DMD, Kim-Schulze S, Huang H-H, Beckmann ND, Nirenberg S, Wang B, Lavin Y, Swartz TH, Madduri D, Stock A, Marron TU, Xie H, Patel M, Tuballes K, Van Oekelen O, Rahman A, Kovatch P, Aberg JA, Schadt E, Jagannath S, Mazumdar M, Charney AW, Firpo-Betancourt A, Mendu DR, Jhang J, Reich D, Sigel K, Cordon-Cardo C, Feldmann M, Parekh S, Merad M, Gnajtic S. 2020. An inflammatory cytokine signature predicts COVID-19 severity and survival. *Nat Med* **26**:1636–1643. <https://doi.org/10.1038/s41591-020-1051-9>.
  168. Varga Z, Flammer AJ, Steiger P, Haberecker M, Andermatt R, Zinkernagel AS, Mehra MR, Schuepbach RA, Ruschitzka F, Moch H. 2020. Endothelial cell infection and endotheliitis in COVID-19. *Lancet* **395**:1417–1418. [https://doi.org/10.1016/S0140-6736\(20\)30937-5](https://doi.org/10.1016/S0140-6736(20)30937-5).
  169. Verger A, Bahloul A, Melki S, Karcher G, Imbert L, Marie P-Y. 2020. Tracheobronchitis signs observed on ventilation lung scintigraphy during the course of COVID-19 infection. *Eur J Nucl Med Mol Imaging* **47**:2709–2710. <https://doi.org/10.1007/s00259-020-04834-7>.
  170. Voiriot G, Dorgham K, Bachelot G, Fajac A, Morand-Joubert L, Parizot C, Gerotziafas G, Farabos D, Trugnan G, Eguether T, Blayau C, Djibré M, Elabbadi A, Gibelin A, Labbé V, Parrot A, Turpin M, Cadranel J, Gorochov G, Fartoukh M, Lamazière A. 2022. Identification of bronchoalveolar and blood immune-inflammatory biomarker signature associated with poor 28-day outcome in critically ill COVID-19 patients. *Sci Rep* **12**:9502. <https://doi.org/10.1038/s41598-022-13179-0>.
  171. Voiriot G, Fajac A, Lopinto J, Labbé V, Fartoukh M. 2020. Bronchoalveolar lavage findings in severe COVID-19 pneumonia. *Intern Emerg Med* **15**:1333–1334. <https://doi.org/10.1007/s11739-020-02356-6>.
  172. Wang D, Hu B, Hu C, Zhu F, Liu X, Zhang J, Wang B, Xiang H, Cheng Z, Xiong Y, Zhao Y, Li Y, Wang X, Peng Z. 2020. Clinical characteristics of 138 hospitalized patients with 2019 novel coronavirus-infected pneumonia in Wuhan, China. *JAMA* **323**:1061–1069. <https://doi.org/10.1001/jama.2020.1585>.
  173. Wauters E, Mol PV, Garg AD, Jansen S, Herck YV, Vanderbeke L, Bassez A, Boeckx B, Malengier-Devlies B, Timmerman A, Van Brussel T, Van Buyten T, Schepers R, Heylen E, Dauwe D, Doods C, Gunst J, Hermans G, Meersseman P, Testelmans D, Yserbyt J, Tejpar S, De Wever W, Matthys P, CONTAGIOUS Collaborators, Neyts J, Wauters J, Qian J, Lambrechts D. 2021. Discriminating mild from critical COVID-19 by innate and adaptive immune single-cell profiling of bronchoalveolar lavages. *Cell Res* **31**:272–290. <https://doi.org/10.1038/s41422-020-00455-9>.
  174. Wendisch D, Dietrich O, Mari T, von Stillfried S, Ibarra IL, Mittermaier M, Mache C, Chua RL, Knoll R, Timm S, Brumhard S, Krammer T, Zauber H, Hiller AL, Pascual-Reguant A, Mothes R, Bülow RD, Schulze J, Leipold AM, Djudjaj S, Erhard F, Geffers R, Pott F, Kazmierski J, Radke J, Pergantis P, Baßler K, Conrad C, Aschenbrenner AC, Sawitzki B, Landthaler M, Wyler E, Horst D, Deutsche COVID-19 OMICS Initiative (DeCOI), Hippenstiel S, Hocke A, Heppner FL, Uhrig A, Garcia C, Machleidt F, Herold S, Elez Kurtaj S, Thibeault C, Witzentrath M, Cochain C, Suttorp N, Drosten C, Goffinet C, Kurth F, Schultze JL, Radbruch H, Ochs M, Eils R, Müller-Redetzky H, Hauser AE, Luecken MD, Theis FJ, Conrad C, Wolff T, Boor P, Selbach M, Saliba AE, Sander LE. 2021. SARS-CoV-2 infection triggers profibrotic macrophage responses and lung fibrosis. *Cell* **184**:6243–6261.e27. <https://doi.org/10.1016/j.cell.2021.11.033>.
  175. Wichmann D, Sperhake J-P, Lütgehetmann M, Steurer S, Edler C, Heinemann A, Heinrich F, Mushumba H, Kniep I, Schröder AS, Burdelski C, de Heer G, Nierhaus A, Frings D, Pfefferle S, Becker H, Bredereke-Wiedling H, de Weerth A, Paschen HR, Sheikhzadeh-Eggers S, Stang A, Schmiedel S, Bokemeyer C, Addo MM, Aepfelbacher M, Püschel K, Kluge S. 2020. Autopsy findings and venous thromboembolism in patients with COVID-19. *Ann Intern Med* **173**:268–277. <https://doi.org/10.7326/M20-2003>.
  176. Wiersinga WJ, Rhodes A, Cheng AC, Peacock SJ, Prescott HC. 2020. Pathophysiology, transmission, diagnosis, and treatment of coronavirus disease 2019 (COVID-19). *JAMA* **324**:782–793. <https://doi.org/10.1001/jama.2020.12839>.
  177. Wilk AJ, Rustagi A, Zhao NQ, Roque J, Martínez-Colón GJ, McKechnie JL, Ivison GT, Ranganath T, Vergara R, Hollis T, Simpson LJ, Grant P, Subramanian A, Rogers AJ, Blish CA. 2020. A single-cell atlas of the peripheral immune response in patients with severe COVID-19. *Nat Med* **26**:1070–1076. <https://doi.org/10.1038/s41591-020-0944-y>.
  178. Winkler ES, Bailey AL, Kafai NM, Nair S, McCune BT, Yu J, Fox JM, Chen RE, Earnest JT, Keeler SP, Ritter JH, Kang LI, Dort S, Robichaud A, Head R, Holtzman MJ, Diamond MS. 2020. SARS-CoV-2 infection of human ACE2-transgenic mice causes severe lung inflammation and impaired function. *Nat Immunol* **21**:1327–1335. <https://doi.org/10.1038/s41590-020-0778-2>.
  179. Witt AN, Green RD, Winterborn AN. 2021. A meta-analysis of rhesus macaques (*Macaca mulatta*), cynomolgus macaques (*Macaca fascicularis*), African green monkeys (*Chlorocebus aethiops*), and ferrets (*Mustela putorius furo*) as large animal models for COVID-19. *Comp Med* **71**:433–441. <https://doi.org/10.30802/AALAS-CM-21-000032>.
  180. Wong HYF, Lam HYS, Fong AH-T, Leung ST, Chin TW-Y, Lo CSY, Lui MM-S, Lee JCY, Chiu KW-H, Chung T, Lee EYP, Wan EYF, Hung IFN, Lam TPW, Kuo MD, Ng MY. 2020. Frequency and distribution of chest radiographic findings in COVID-19-positive patients. *Radiology* **296**:E72–E78. <https://doi.org/10.1148/radiol.2020201160>.
  181. Wong L-YR, Zheng J, Wilhelmsen K, Li K, Ortiz ME, Schnicker NJ, Thurman A, Pezzulo AA, Szachowicz PJ, Li P, Pan R, Klumpp K, Aswad F, Rebo J, Narumiya S, Murakami M, Zuniga S, Sola I, Enjuanes L, Meyerholz DK, Fortney K, McCray PB Jr, Perlman S. 2022. Eicosanoid signalling blockade protects middle-aged mice from severe COVID-19. *Nature* **605**:146–151. <https://doi.org/10.1038/s41586-022-04630-3>.
  182. Woolsey C, Borisevich V, Prasad AN, Agans KN, Deer DJ, Dobias NS, Heymann JC, Foster SL, Levine CB, Medina L, Melody K, Geisbert JB, Fenton KA, Geisbert TW, Cross RW. 2021. Estab-

- lishment of an African green monkey model for COVID-19 and protection against reinfection. *Nat Immunol* 22:86–98. <https://doi.org/10.1038/s41590-020-00835-8>.
183. Wu C, Chen X, Cai Y, Xia J, Xing Z, Xu S, Huang H, Zhang L, Xia Z, Du C, Zhang Y, Song J, Wang S, Chao Y, Yang Z, Xu J, Zhou X, Chen D, Xiong W, Xu L, Zhou F, Jiang J, Bai C, Zheng J, Song Y. 2020. Risk factors associated with acute respiratory distress syndrome and death in patients with coronavirus disease 2019 pneumonia in Wuhan, China. *JAMA Intern Med* 180:934–943. <https://doi.org/10.1001/jamainternmed.2020.0994>.
184. Peng W, Chen D, Ding W, Ping W, Hou H, Bai Y, Zhou Y, Li K, Xiang S, Liu P, Ju J, Guo E, Liu J, Yang B, Fan J, He L, Sun Z, Feng L, Wang J, Wu T, Wang H, Cheng J, Xing H, Meng Y, Li Y, Zhang Y, Luo H, Xie G, Lan X, Tao Y, Li J, Yuan H, Huang K, Sun W, Qian X, Li Z, Huang M, Ding P, Wang H, Qiu J, Wang F, Wang S, Zhu J, Ding X, Chai C, Liang L, Wang X, Luo L, Sun Y, Yang Y, Zhuang Z, Li T, Tian L, Zhang S, Zhu L, Chang A, Chen L, Wu Y, Ma X, Chen F, Ren Y, Xu X, Liu S, Wang J, Yang H, Wang L, Sun C, Ma D, Jin X, Chen G. 2021. The trans-omics landscape of COVID-19. *Nat Commun* 12:4543. <https://doi.org/10.1038/s41467-021-24482-1>.
185. Wu Z, McGoogan JM. 2020. Characteristics of and important lessons from the coronavirus disease 2019 (COVID-19) outbreak in China. *JAMA* 323:1239–1242. <https://doi.org/10.1001/jama.2020.2648>.
186. Xu Z, Shi L, Wang Y, Zhang J, Huang L, Zhang C, Liu S, Zhao P, Liu H, Zhu L, Tai Y, Bai C, Gao T, Song J, Xia P, Dong J, Zhao J, Wang FS. 2020. Pathological findings of COVID-19 associated with acute respiratory distress syndrome. *Lancet Respir Med* 8:420–422. [https://doi.org/10.1016/S2213-2600\(20\)30076-X](https://doi.org/10.1016/S2213-2600(20)30076-X).
187. Yang X, Yu Y, Xu J, Shu H, Xia J, Liu H, Wu Y, Zhang L, Yu Z, Fang M, Yu T, Wang Y, Pan S, Zou X, Yuan S, Shang Y. 2020. Clinical course and outcomes of critically ill patients with SARS-CoV-2 pneumonia in Wuhan, China: A single-centered, retrospective, observational study. *Lancet Respir Med* 8:475–481. [https://doi.org/10.1016/S2213-2600\(20\)30079-5](https://doi.org/10.1016/S2213-2600(20)30079-5).
188. Yao X-H, He Z-C, Li T-Y, Zhang H-R, Wang Y, Mou H, Guo Q, Yu S-C, Ding Y, Liu X, Ping YF, Bian XW. 2020. Pathological evidence for residual SARS-CoV-2 in pulmonary tissues of a ready-for-discharge patient. *Cell Res* 30:541–543. <https://doi.org/10.1038/s41422-020-0318-5>.
189. Yinda CK, Port JR, Bushmaker T, Owusu IO, Purushotham JN, Avanzato VA, Fischer RJ, Schulz JE, Holbrook MG, Hebner MJ, Rosenke R, Thomas T, Marzi A, Best SM, de Wit E, Shaia C, van Doremalen N, Munster VJ. 2021. K18-hACE2 mice develop respiratory disease resembling severe COVID-19. *PLoS Pathog* 17:e1009195. <https://doi.org/10.1371/journal.ppat.1009195>.
190. Yu P, Qi F, Xu Y, Li F, Liu P, Liu J, Bao L, Deng W, Gao H, Xiang Z, Xiao C, Lv Q, Gong S, Liu J, Song Z, Qu Y, Xue J, Wei Q, Liu M, Wang G, Wang S, Yu H, Liu X, Huang B, Wang W, Zhao L, Wang H, Ye F, Zhou W, Zhen W, Han J, Wu G, Jin Q, Wang J, Tan W, Qin C. 2020. Age-related rhesus macaque models of COVID-19. *Animal Model Exp Med* 3:93–97. <https://doi.org/10.1002/ame2.12108>.
191. Yuan L, Zhu H, Zhou M, Ma J, Chen R, Yao C, Chen L, Wu K, Cai M, Hong J, Li L, Liu C, Yu H, Zhang Y, Wang J, Zhang T, Ge S, Zhang J, Yuan Q, Chen Y, Tang Q, Chen H, Cheng T, Guan Y, Xia N. 2021. Gender associates with both susceptibility to infection and pathogenesis of SARS-CoV-2 in Syrian hamster. *Signal Transduct Target Ther* 6:136. <https://doi.org/10.1038/s41392-021-00552-0>.
192. Zeng Z, Xu L, Xie X, Yan H, Xie B, Xu W, Liu X, Kang G, Jiang W, Yuan J. 2020. Pulmonary pathology of early-phase COVID-19 pneumonia in a patient with a benign lung lesion. *Histopathology* 77:823–831. <https://doi.org/10.1111/his.14138>.
193. Zhang AJ, Lee AC-Y, Chu H, Chan JF-W, Fan Z, Li C, Liu F, Chen Y, Yuan S, Poon VK-M, Chan CC, Cai JP, Wu KL, Sridhar S, Chan YS, Yuen KY. 2021. SARS-CoV-2 infects and damages the mature and immature olfactory sensory neurons of hamsters. *Clin Infect Dis* 73:e503–e512. <https://doi.org/10.1093/cid/ciaa995>.
194. Zhang F, Mears JR, Shakib L, Beynor JI, Shanaj S, Korsunsky I, Nathan A, Donlin LT, Raychaudhuri S. 2021. IFN $\gamma$  and TNF $\alpha$  drive a CXCL10<sup>+</sup>CCL2<sup>+</sup> macrophage phenotype expanded in severe COVID-19 lungs and inflammatory diseases with tissue inflammation. *Genome Med* 13:64. <https://doi.org/10.1186/s13073-021-00881-3>.
195. Zhang H, Zhou P, Wei Y, Yue H, Wang Y, Hu M, Zhang S, Cao T, Yang C, Li M, Guo G, Chen X, Chen Y, Lei M, Liu H, Zhao J, Peng P, Wang CY, Du R. 2020. Histopathologic changes and SARS-CoV-2 immunostaining in the lung of a patient with COVID-19. *Ann Intern Med* 172:629–632. <https://doi.org/10.7326/M20-0533>.
196. Zheng H, Li H, Guo L, Liang Y, Li J, Wang X, Hu Y, Wang L, Liao Y, Yang F, Li Y, Fan S, Li D, Cui P, Wang Q, Shi H, Chen Y, Yang Z, Yang J, Shen D, Cun W, Zhou X, Dong X, Wang Y, Chen Y, Dai Q, Jin W, He Z, Li Q, Liu L. 2020. Virulence and pathogenesis of SARS-CoV-2 infection in rhesus macaques: A nonhuman primate model of COVID-19 progression. *PLoS Pathog* 16:e1008949. <https://doi.org/10.1371/journal.ppat.1008949>.
197. Zheng J, Wong L-YR, Li K, Verma AK, Ortiz ME, Wohlford-Lenane C, Leidinger MR, Knudson CM, Meyerholz DK, McCray PB, Perlman S. 2021. COVID-19 treatments and pathogenesis including anosmia in K18-hACE2 mice. *Nature* 589:603–607. <https://doi.org/10.1038/s41586-020-2943-z>.
198. Zhou P, Yang X-L, Wang X-G, Hu B, Zhang L, Zhang W, Si H-R, Zhu Y, Li B, Huang C-L, Chen HD, Chen J, Luo Y, Guo H, Jiang RD, Liu MQ, Chen Y, Shen XR, Wang X, Zheng XS, Zhao K, Chen QJ, Deng F, Liu LL, Yan B, Zhan FX, Wang YY, Xiao GF, Shi ZL. 2020. A pneumonia outbreak associated with a new coronavirus of probable bat origin. *Nature* 579:270–273. <https://doi.org/10.1038/s41586-020-2012-7>.
199. Zhou Z, Ren L, Zhang L, Zhong J, Xiao Y, Jia Z, Guo L, Jing Y, Wang C, Jiang S, Yang D, Zhang G, Li H, Chen F, Xu Y, Chen M, Gao Z, Yang J, Dong J, Liu B, Zhang X, Wang W, He K, Jin Q, Li M, Wang J. 2020. Heightened innate immune responses in the respiratory tract of COVID-19 patients. *Cell Host Microbe* 27:883–890.e2. <https://doi.org/10.1016/j.chom.2020.04.017>.
200. Ziehr DR, Alladina J, Petri CR, Maley JH, Moskowitz A, Medoff BD, Hibbert KA, Thompson BT, Hardin CC. 2020. Respiratory pathophysiology of mechanically ventilated patients with COVID-19: A cohort study. *Am J Respir Crit Care Med* 201:1560–1564. <https://doi.org/10.1164/rccm.202004-1163LE>.
201. Zuo Y, Warnock M, Harbaugh A, Yalavarthi S, Gockman K, Zuo M, Madison JA, Knight JS, Kanthi Y, Lawrence DA. 2021. Plasma tissue plasminogen activator and plasminogen activator inhibitor-1 in hospitalized COVID-19 patients. *Sci Rep* 11:1580. <https://doi.org/10.1038/s41598-020-80010-z>.